SKB

TECHNICAL REPORT 92-36

On the interpretation of double-packer tests in heterogeneous porous media:

Numerical similations using the stochastic continuum analogue

Sven Follin

Department of Engineering Geology, Lund University,
Lund, Sweden

December 1992

SVENSK KÄRNBRÄNSLEHANTERING AB
SWEDISH NUCLEAR FUEL AND WASTE MANAGEMENT CO

BOX 5864 S-102 48 STOCKHOLM

TEL 08-665 28 00 TELEX 13108 SKB S
TELEFAX 08-661 57 19

ON THE INTERPRETATION OF DOUBLE-PACKER TESTS IN HETEROGENEOUS POROUS MEDIA: NUMERICAL SIMULATIONS USING THE STOCHASTIC CONTINUUM ANALOGUE

Sven Follin

Department of Engineering Geology, Lund University, Lund, Sweden

December 1992

ON THE INTERPRETATION OF DOUBLE-PACKER TESTS IN HETEROGENEOUS POROUS MEDIA:

Numerical simulations using the stochastic continuum analogue

SVEN FOLLIN

December 1992

Department of Engineering Geology
Lund University, Sweden

KEYWORDS: HETEROGENEITY, SUPPORT SCALE, DOUBLE-PACKER TESTING, SIMULATION

Preface

The idea of simulating double-packer tests in heterogeneous porous media arose during meetings and discussions conducted by SKB - the Swedish Nuclear Fuel and Waste Management Company in conjunction with the SKB 91 and the Äspö Hard Rock Laboratory projects. The far-field hydraulic modelling undertaken in these two projects is mainly performed with two computer codes called HYDRASTAR and PHOENICS, respectively, which both use heterogeneous porous media concepts.

Two important constraints shared by the two modelling scenarios are the limited amount of hydraulic conductivity data for the model set-up, and the huge volumes of rock being modelled. Typically, it has been necessary to resort to single-hole measurements such as fixed-interval double-packer tests. The body of these tests are carried out with short test section lengths (straddle intervals). Accordingly, the data used for far-field modelling have been regularised (scaled-up) in order to fit the comparatively coarser numerical discretisation. The objectives of this study are to closely examine the support scale of double-packer tests and to discuss some tentative possibilities to improve present interpretation, regularisation and modelling techniques based on the stochastic continuum analogue.

The transmissivity value determined with a double-packer test depends to some extent on the interpretation method used, and the interpretation procedure is therefore a debatable subject. As a natural consequence of the support scale studies, some of the methods used for interpreting constant-head injection tests within the Swedish nuclear waste repository programme are compared and ambiguities observed in relation to real tests are discussed.

The author is grateful for the financial support from [illegible] the valuable comments of Mr. Jan-Erik Andersson, GEOSIGMA, Mr. Joel [illegible], GOLDER GEOSYSTEM, Dr. J. Jaime Gómez-Hernández, UPV, Dr. Roger Thunvik, KTH, Dr. Clifford Voss, USGS, and Mr. Anders Winberg, CONTERRA.

Abstract (English)

Flow in fractured crystalline (hard) rocks is of interest in Sweden for assessing the post-closure radiological safety of a deep repository for high-level nuclear waste. Depending on the scale of the problem under study different modelling concepts are used. For simulation of flow and mass transport in the far field different porous media concepts are often used, whereas discrete fracture/channel network concepts are often used for near-field simulations. Due to lack of data, it is generally necessary to have resort to single-hole double-packer test data for the far-field simulations, i.e., test data on a small scale are regularised in order to fit a comparatively coarser numerical discretisation, which is governed by various computational constraints. It is interesting to note that single-hole fixed-interval packer test data are also used as the basis for derivation of the hydrogeologic properties of discrete fracture models, despite the different assumptions regarding the geometry of flow. Obviously, techniques that improve the interpretation and the regularisation of single-hole double-packer tests are of paramount interest. In the present study the Monte Carlo method is used to investigate the relationship between the transmissivity value interpreted and the corresponding radius of influence in conjunction with single-hole double-packer tests in heterogeneous formations. The numerical flow domain is treated as a two-dimensional heterogeneous porous medium with a spatially varying diffusivity on a 3 m scale. Two methods which have been traditionally used for interpreting constant-head injection tests within the Swedish nuclear waste repository programme, namely Moye's and Jacob-Lohman's formulae, are compared and ambiguities observed in relation to real tests are discussed. The Monte Carlo simulations demonstrate the sensitivity to the correlation range of a spatially varying diffusivity field. In contradiction to what is tacitly assumed in stochastic subsurface hydrology, the results show that the lateral support scale (e.g., the radius of influence) of transmissivity measurements in heterogeneous porous media is a random variable, which is affected by both the hydraulic and statistical characteristics. If these results are general, the traditional methods for scaling-up, assuming a constant lateral scale of support and a multinormal distribution, may lead to an underestimation of the persistence and connectivity of transmissive zones, particularly in highly heterogeneous porous media.

Abstract (Swedish)

Kunskap om grundvattnets strömning i sprickigt berg är av betydelse för säkerhetsanalyser rörande djupförvaring av utbränt kärnbränsle. Olika typer av grundvattenmodeller förekommer beroende på beräkningsskalan storlek. För fjärrzonsberäkningar antas ofta att berget kan modelleras som om det vore ett poröst medium. För närzonsberäkningar används även sprickmodeller. Bristen på indata i lämplig skala i samband med fjärrzonsberäkningar medför att man ofta tvingas skala upp s.k. enhålsmätningar till aktuell beräkningsskala. Enhålsmätningar i liten skala förekommer i stora mängder och används även för att kalibrera sprickmodeller vid närzonsberäkningar. Med tanke på enhålsmätningarnas relativt sett stora betydelse finns det anledning att se över tolknings-, kalibrerings- och uppskalningskoncepten. I denna rapport använder vi Monte Carlo metoden för att undersöka influensradiens relation till tolkat transmissivitetsvärde i samband med enhålsmätningar i starkt heterogena och porösa media. Två tolkningsmetoder som används i Sverige inom forskningen för djupförvaring av använt kärnbränsle för att tolka s.k. vatteninjektionsmätningar vid konstant tryck (Moye och Jacob-Lohman) ligger till grund för de beräkningsresultat som redovisas. Beräkningsresultaten visar att influensradien inte är konstant utan att denna beror både på de hydrauliska och statistiska egenskaperna hos det omgivande mediet. Detta innebär att de uppskalningsalgoritmer som traditionellt används underskattar uthålligheten och konnektiviteten hos småskaliga strukturer med hög transmissivitet.

Contents

Chapter 1

Introduction

Depending on the scale of the problem under study different modelling concepts are used in Sweden for assessing the post-closure radiological safety of a deep repository for high-level nuclear waste in fractured crystalline (hard) rocks. For simulation of flow and mass transport in the far field different porous media concepts are often used, whereas discrete fracture/channel network concepts are often used for near-field simulations. Due to lack of data, it is generally necessary to have resort to single-hole double-packer test data for far-field simulations. That is to say, test data on a small scale are regularised in order to fit a comparatively coarser numerical discretisation (see, e.g., Gustafson *et al.*, 1989; Svensson, 1991; Norman, 1992), which is governed by various computational constraints. It is interesting to note that single-hole fixed-interval packer test data are also used as the basis for derivation of the hydrogeologic properties of discrete fracture models, despite the different assumptions regarding the geometry of flow (see, e.g., Geier and Axelsson, 1991; Geier *et al.*, 1992). Obviously, techniques that improve the interpretation and the regularisation of single-hole double-packer tests are of paramount interest.

The present study attempts to address and support the early stages of hydrogeologic characterisation for a high-level radioactive-waste repository in fractured hard rocks using the stochastic continuum analogue on a 3 m scale. Thus, the main assumption made in this study is that fractured hard rocks can be treated as highly heterogeneous porous media on the scale of interest. The Monte Carlo method is used to investigate the relationship between the transmissivity value interpreted and the corresponding radius of influence for single-hole double-packer tests. The objective is to closely examine the lateral support scale (e.g., the radius of influence) of double-packer tests and to discuss some tentative possibilities to improve present interpretation, regularisation and modelling techniques. The interest for single-hole double-packer tests reflects the likelihood that the early screening of the rock mass will be conducted with a limited number of boreholes; the best use of the drilling resources will likely require distributing boreholes over a large area, rather than concentrating them in the small area that would be useful for interference testing. Single-hole testing is thus likely to be one of the primary methods for investigating the hydrogeologic properties of the rock mass.

This study simulates one of the more frequently test methods used, namely the constant-head injection test, and examines numerically its application to transient groundwater flow in a confined two-dimensional slab of porous rock, see Figure 1. Hence, the present study deals with a highly heterogeneous porous medium in two dimensions which has a spatially varying diffusivity. The spatial variability is assumed to be multinormal on a 3 m scale. Two methods which have been used for interpreting constant-head injection tests within the Swedish nuclear waste repository programme, namely Moye's and Jacob-Lohman's methods, are compared and ambiguities observed in relation to real double-packer tests are discussed. The recovery portion of a constant-head injection test is not simulated in this study, although it is used within the Swedish nuclear waste repository programme (see, e.g., Nilsson, 1989, 1990). However, we argue that Cooper-Jacob's method, which is the method used for interpreting the recovery portion, is constrained by the same assumptions about the flow regime as the Jacob-Lohman method.

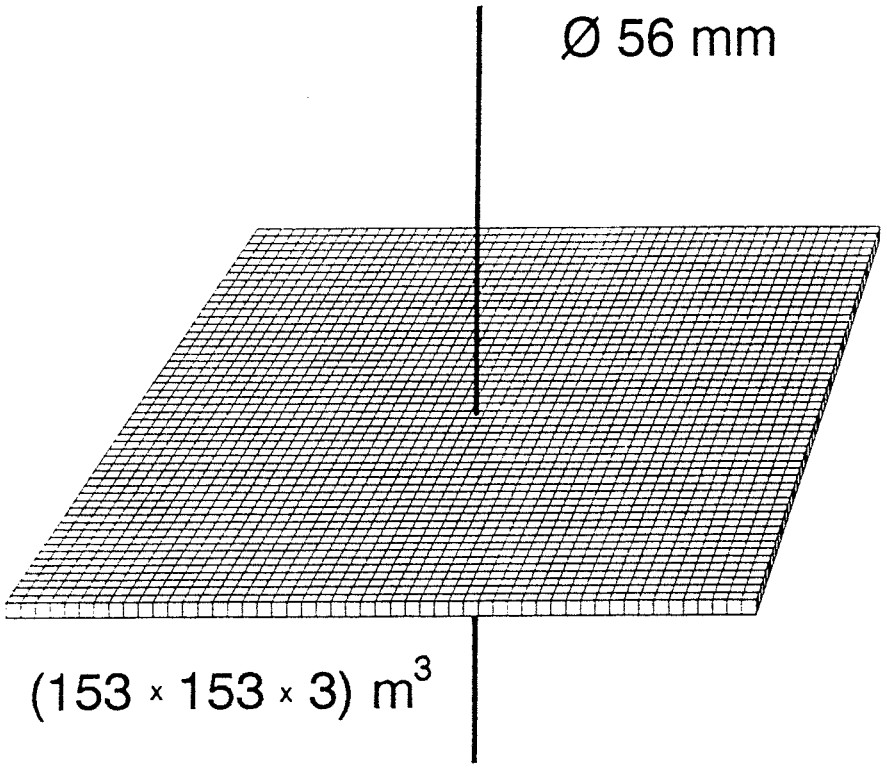

Fig. 1 Perspective view of the borehole and the grid geometry of the numerical flow domain. The thickness of the horizontal slab is conceptual. The heterogeneity generated corresponds to the statistics of transmissivity measurements made in slim core boreholes on a 3 m scale.

Chapter 2

Review of theory

In transient groundwater flow, the mass balance equation for a control volume of a saturated porous medium becomes

$$\frac{\partial}{\partial t}(\phi \rho_w) + \nabla \cdot (\rho_w \vec{q}) = 0 \tag{1}$$

where ϕ is the effective porosity of the porous medium, ρ_w is the density of the groundwater, and $\vec{q}$ is the volumetric groundwater flow (flux). For the general case of an anisotropic porous medium the flux is given by Darcy's law, which can be written as

$$\vec{q} = - \frac{\tilde{k}}{\mu_w} (\nabla p_w + \rho_w g \hat{z}) \tag{2}$$

where $\tilde{k}$ is the intrinsic permeability tensor of the porous medium, μ_w is the dynamic viscosity of the groundwater, p_w is the pressure of the groundwater, g is the acceleration due to gravity, and $\hat{z}$ is the vertical unit vector pointing upwards. If the porous medium is of constant porosity and its intrinsic permeability is isotropic and homogeneous, and if the groundwater density and viscosity are constant, a combination of the mass balance equation and Darcy's law can be written as

$$\nabla^2 h = \frac{S_s}{K} \frac{\partial h}{\partial t} \tag{3}$$

which is known as the diffusion equation. In equation (3), h denotes the hydraulic head, which is defined as $h = (p_w / \rho_w g) + \Delta z$, where Δz is the elevation head from a given datum. S_s is the specific storage coefficient, which is a material property of the porous medium and represents the volume of groundwater that a unit volume of the aquifer releases from storage for a unit decline in hydraulic head. K is the hydraulic conductivity

of the aquifer and is a material property of both the porous medium and the fluid. For the special case of horizontal transient flow in a confined two-dimensional aquifer of constant thickness b, equation (3) simplifies to

$$\frac{\partial^2 h}{\partial x^2} + \frac{\partial^2 h}{\partial y^2} = \frac{S}{T}\frac{\partial h}{\partial t} \tag{4}$$

where $S = S_s b$ and $T = Kb$. S and T denote the storativity and transmissivity of the aquifer, respectively. Equation (4) is the equation considered in this study, however, for a heterogeneous porous medium with a spatially varying diffusivity T/S, i.e., in the numerical flow model, the spatially varying diffusivity is constant valued within each element.

The flow geometry associated with equation (4) is radial; the flow lines radiate in all directions perpendicular to the hole axis. In a homogeneous porous medium, radial flow occurs in well tests where the entire thickness of aquifer lies within the test zone; a fully penetrating well. Classical interpretation methods for well tests in aquifers generally assume a homogeneous porous medium and simple flow geometries such as linear, radial, and spherical flow, see Figure 2a. Recently, the concept of fractional dimensions (Barker, 1988) has been introduced for interpreting hydraulic tests, see Figure 2b. In Sweden, fractional dimension analyses have so far been applied to test data from Stripa (Doe and Geier, 1990) and from Finnsjön (Geier and Axelsson, 1991; Geier and Doe, 1992).

It is important to note that well tests measure transmissivity and not hydraulic conductivity K. For a fully penetrating well in a homogeneous porous medium, the average hydraulic conductivity is calculated from the transmissivity by taking b as the thickness of the aquifer, i.e., $K = T/b$. However, for borehole tests such as the constant-head injection test, b is not readily defined. This is particular true for the short packer spacings commonly used to calculate the hydraulic conductivity of hard rocks in Sweden, where packer spacings of the order of a few metres (or less) have been used at several sites such as Finnsjön, Stripa, and Äspö (see, e.g., Carlsson *et al.*, 1980; Holmes, 1989; Nilsson, 1989, 1990).

Traditionally, the b used for calculating the hydraulic conductivity in conjunction with a constant-head injection test is simply the packer spacing L between the double-packers, despite facts such as (*i*) the test section covers only a small portion of total thickness of the rock tested and (*ii*) only a small portion of the test section is conducting fluid, i.e., groundwater flow takes place in the fractures intersecting the test section.

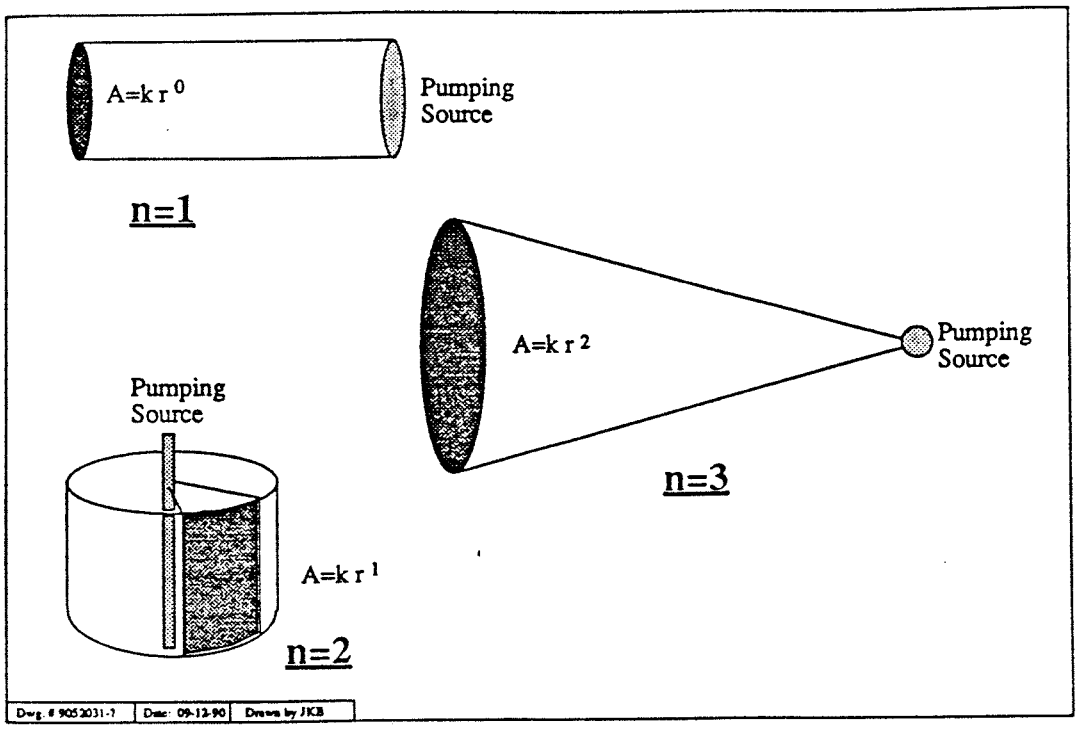

Fig. 2a Schematic view of integer-value flow geometries; linear, radial, and spherical flow (reproduced from Ball *et al.*, 1992).

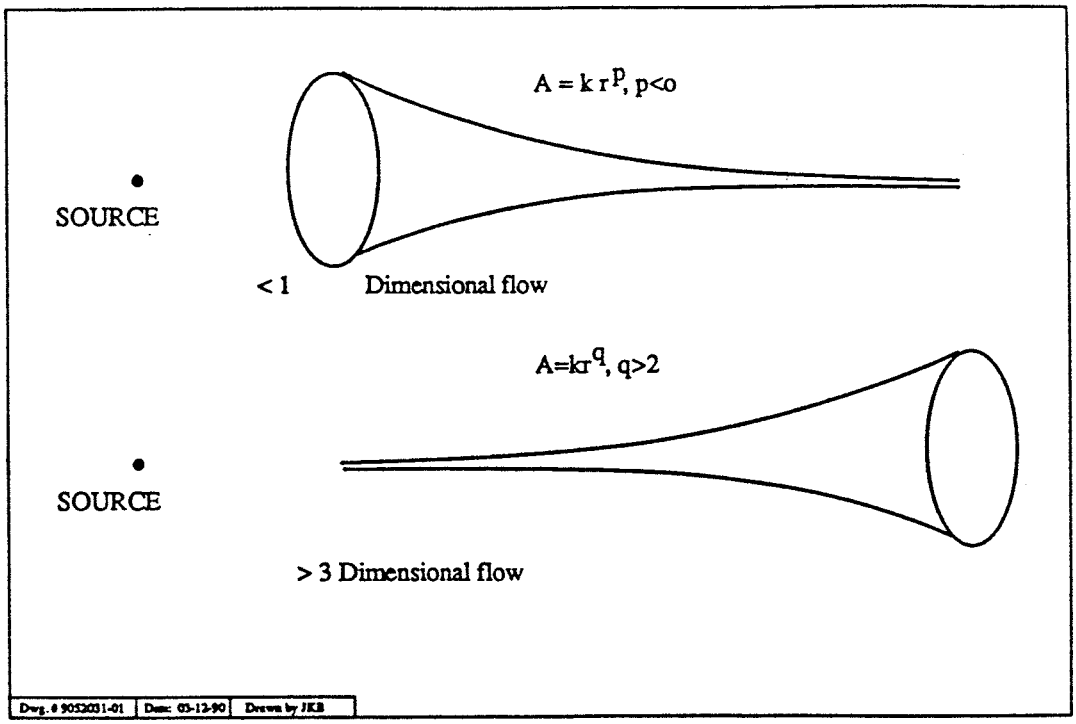

Fig. 2b Schematic view of flow geometries with fractional dimensions, i.e., dimensions intermediate to the integer-value dimensions (reproduced from Ball *et al.*, 1992).

Groundwater flow and mass transport in fractured hard rocks occur in fractures planes. The intuitive way to model flow and transport in such a system is to use a fracture or channel network analogue (see, e.g., Long *et al.*, 1982; Robinson, 1984; Dershowitz, 1985; Cacas *et al.*, 1990a,b; Dverstorp, 1991). However, due to the severe computational constraints caused by the scale of the problem relative the kind of information that is required for setting up a representative fracture flow geometry, different continuum approximations are frequently used for modelling far-field groundwater flow and mass transport in fractured hard rocks.

The single-porosity approximation (Hubbert, 1956; Bear, 1972) and double-porosity approximation (Barenblatt *et al.*, 1960; Warren and Root, 1963, Duguid and Lee, 1977) represent so called deterministic continuum approaches. The approach adopted in this study is the stochastic continuum method (Neuman 1987, 1988), which can be looked upon as an alternative to both the traditional effective porous medium concept and the discrete fracture or channel analogue. Neuman (1988) advocated that packer spacings which exceed the mean spacing of coated fractures by not more than one order of magnitude should yield data amenable to treatment by the stochastic continuum method on that scale in most hard rocks.

In Figures 3 and 4, transmissivities from one of the boreholes at Äspö Hard Rock Laboratory are shown. The fixed-interval contant-head injection tests were run for 10 minutes (cf. Nilsson, 1989). The test section length (packer spacing) was 3 m, and the interpretations were made with Moye's formula (Moye, 1967), which can be written as

$$T_m = \frac{Q(t)}{H}\left[\frac{1 + ln(L/2\,r_w)}{2\,\pi}\right] \tag{5}$$

where T_m is Moye's transmissivity, $Q(t)$ is the volumetric flow rate of water at the end of the injection period, H is the excess injection head, L is the length of the test section, and r_w is the borehole radius. A description of the test procedure used in Sweden in conjunction with constant-head injection tests and Moye's formula is found in, e.g., Almén *et al.* (1986) and Andersson *et al.* (1988). Moye's formula assumes:

- porous medium
- steady-state flow
- homogeneous hydraulic conductivity
- cylindrical flow near the well and spherical flow at a distance which is related to the length of the test section (packer spacing).

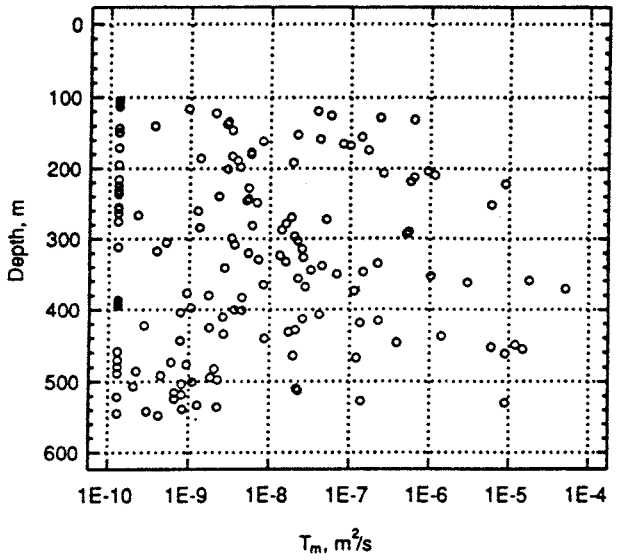

Fig. 3 Plot of 3 m transmissivities vs. depth for borehole KAS03 at Äspö Hard Rock Laboratory. The transmissivities are computed with Moye's formula. t = 10 minutes.

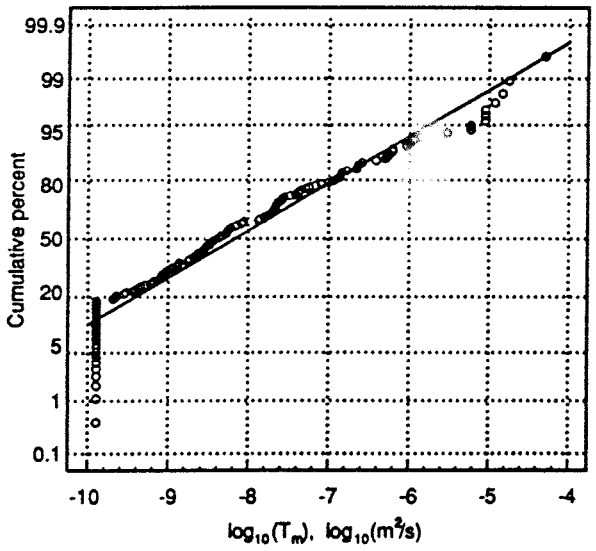

Fig. 4 Normal probability plot of 3 m transmissivities for borehole KAS03 at Äspö Hard Rock Laboratory. The transmissivities are computed with Moye's formula. t = 10 minutes.

Braester and Thunvik (1982, 1984) compared Moye's formula (and Hvorslev's formula, which is also commonly used in geotechnical practice) with an analytical solution derived by Dagan (1978) and with a numerical solution of their own. A few of their conclusions are of interest for the present study, among others, that:

- conductivity heterogeneities in the region below and above the packers have no significant influence on the calculated conductivity of the tested section between the packers
- a low conductivity region close to the borehole due to, e.g., mechanical clogging and chemical scaling distorts significantly the representative conductivity of the rock mass
- Moye's formula is dominantly a two-dimensional flow equation, where the errors due to spherical flow result in the derived conductivity being an overestimate, see Figure 5
- Moye's formula may be applied also to discontinuous media, despite the fact that the flow pattern in the two types of media are widely different.

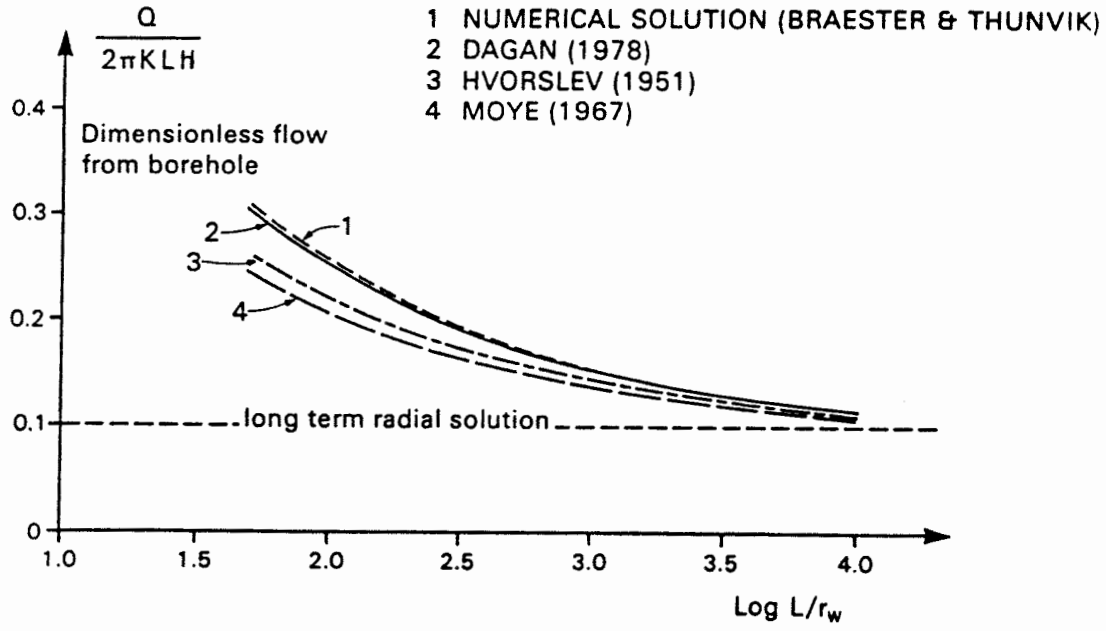

Fig. 5 Spherical flow effects as a function of borehole radius and test zone length for constant-head tests (reproduced from Black and Barker (1987) who refer to Braester and Thunvik, 1984).

The conclusion of Braester and Thunvik (1982, 1984) that a vertical heterogeneity has no significant influence on the calculated transmissivity of the tested rock between the packers is interesting. However, it may be an artifact of studying an axi-symmetric flow domain, i.e., the authors studied steady-state flow from a well into a formation of layered heterogeneity. Hence, in order to be more conclusive on this issue a model that simulates three-dimensional flow in a formation of more irregular heterogeneity is required.

Figure 5 shows spherical flow effects for various test section lengths at steady-state flow. It implies that spherical flow effects increase for $log_{10}(L/r_w) \leq 4$, but that the phenomenon is comparatively unimportant. Nevertheless, one may still argue that the two-dimensional flow domain used in this study is debatable because a test section length of 3 m and a borehole radius of 0.028 m yields that $log_{10}(L/r_w) \approx 2$ and $Q/2\pi T_m H \approx 0.2$.

There are two pertinent conditions that may justify a two-dimensional flow model for studying the support scale of double-packer tests. Firstly, the flow regime of a double-packer test with a short test section length is probably radial at early times rather than spherical. Secondly, vertical boreholes intersect predominantly horizontal structures. As an alternative to the tacit assumption that fractures can be treated as homogeneous planar structures, the numerical flow model used in this study can also be used for studying flow in a heterogeneous fracture plane (cf. Tsang and Tsang, 1989).

Chapter 3

Numerical flow model

The purpose of the numerical flow model is to simulate the hydraulic response in space and time of a constant-head injection test between a pair of packers. The boundary conditions for this kind of test is readily simulated with a Dirichlet condition at the position of the borehole, i.e., a prescribed head corresponding to the excess injection head. The Galerkin formulation of the finite element method to the chosen equation of groundwater flow - equation (4) - is used together with a backward difference formulation to the time derivative of the hydraulic head. In other words, the final formulation results in a system of equations that can be written in matrix form as

$$\left([C] + \Delta t\, [K] \right) \{h\}_{t+\Delta t} = [C]\, \{h\}_t + \Delta t\, \{F\}_{t+\Delta t} \qquad (6)$$

where $[C]$ and $[K]$ are the capacitance and conductance matrices, respectively, $\{h\}$ is the hydraulic head matrix, t is time, and $\{F\}$ is the specified flow matrix.

In Figures 6-8, the parameter grid and the finite element mesh are shown. The conceptual area of the numerical flow domain is $(153\ \text{m})^2$ corresponding to 2,601 $(3\ \text{m})^2$ blocks, see Figure 6. The finite element mesh consists of 5,472 bi-quadratic quadrilaterals (9 node Lagrangian family) and the numerical integration is made with 9 Gauss integration nodes. The total number of nodes is 22,192. The innermost grid block is discretised into 252 elements, see Figure 7, and has a hole in the centre representing the borehole (cf. Figure 1). The borehole radius is about 0.028m, see Figure 8, which equals the nominal borehole radius of the core drillings used within the Swedish nuclear waste repository programme.

A logarithmic time step of $ln(t_{n+1}/t_n) = ln(10)/5$ is used, i.e., five observations per log_{10} time cycle. Equation (6) is solved with a front solver (Duff, 1981). During the simulations the hydraulic head value of the boundary nodes on the borehole perimeter is fixed to 20 m, see Figure 8, which equals the excess injection head used within the Swedish nuclear waste repository programme. The recovery period that follows after a terminated constant-head injection test is not simulated in this study.

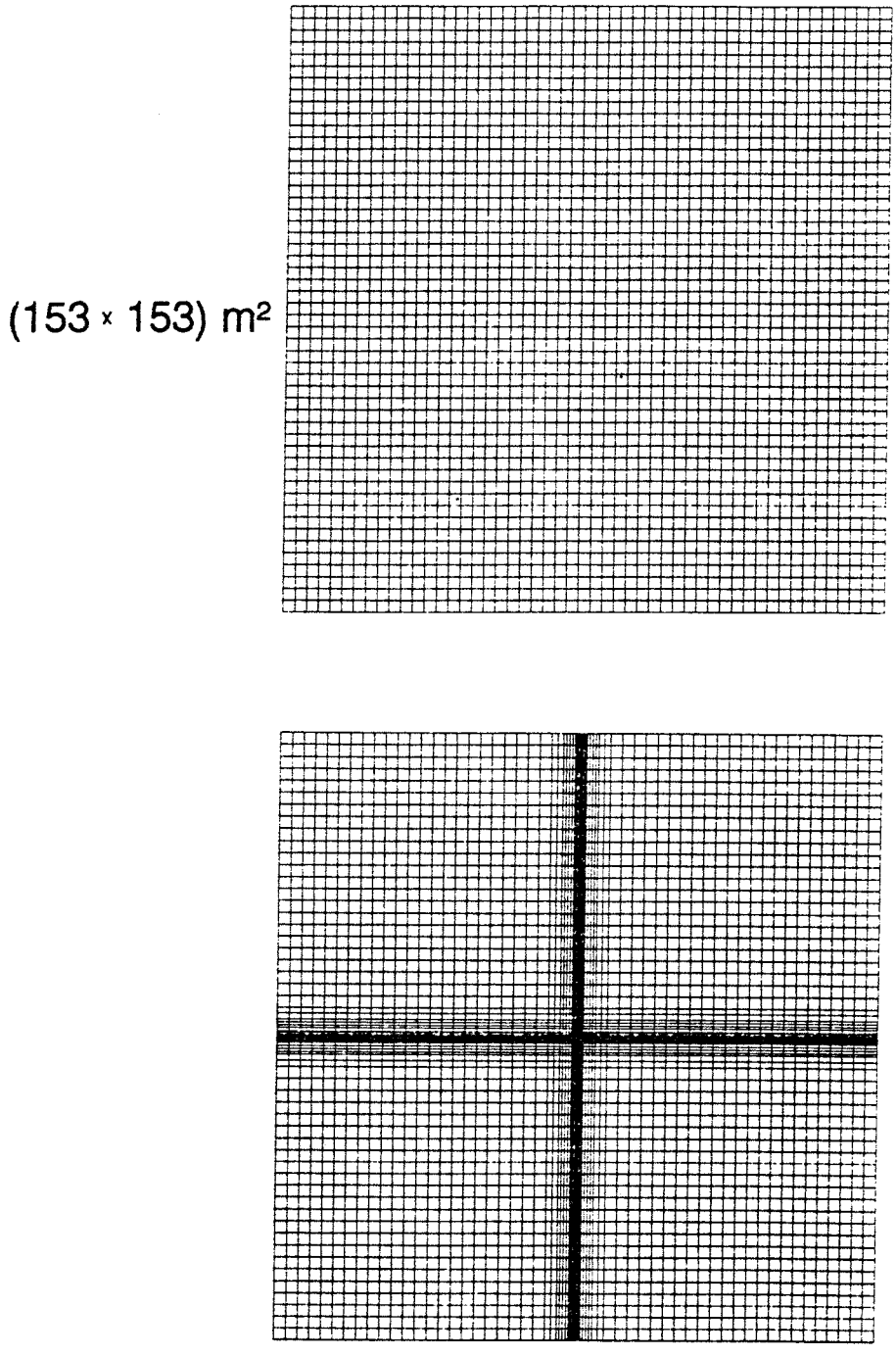

Fig. 6 The parameter grid (top) and the finite element mesh (bottom).

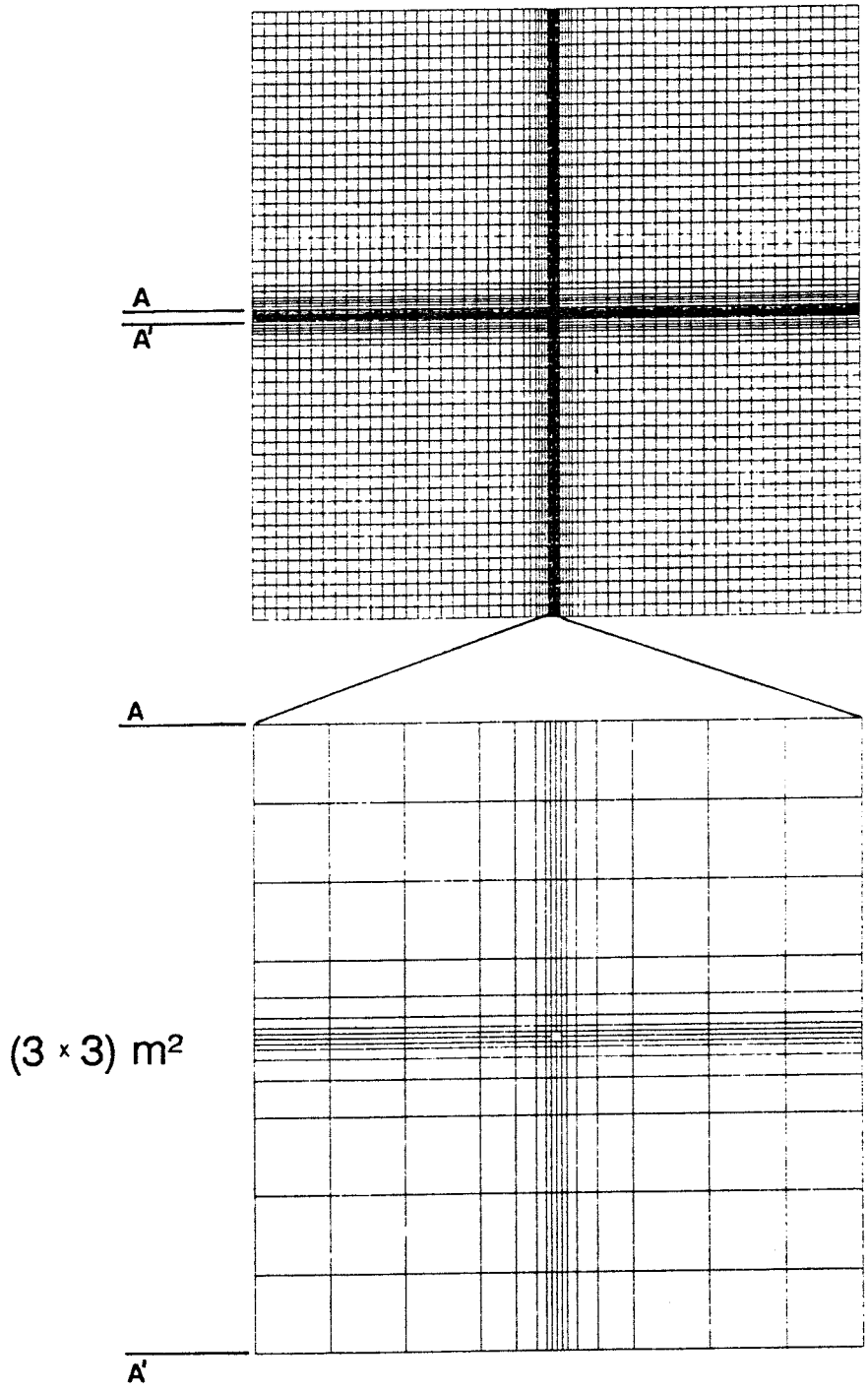

Fig. 7 The finite element mesh (top) and the discretisation of the innermost grid block (bottom).

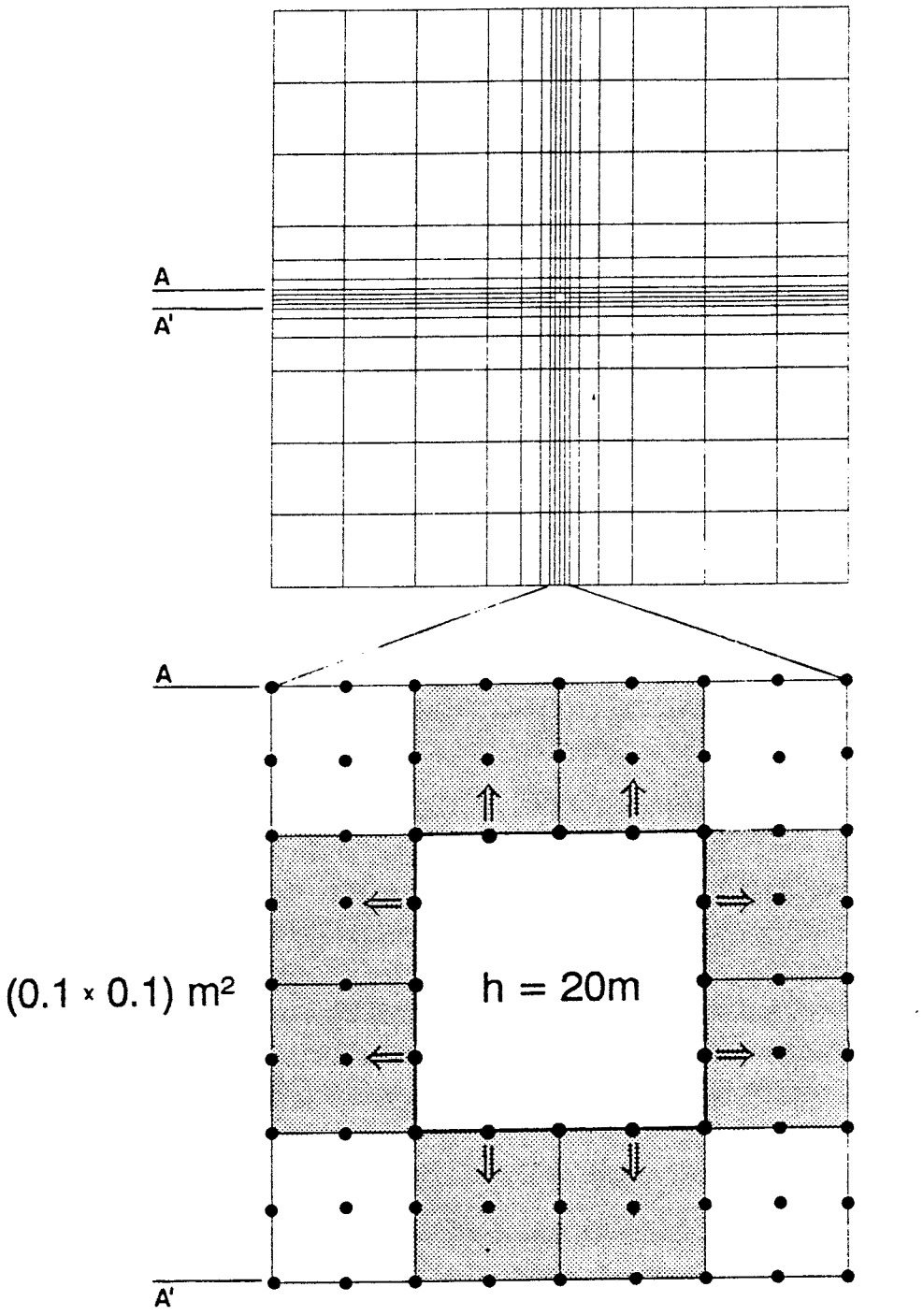

Fig. 8 The discretisation of the innermost grid block (top) and the 16 nodes defining the borehole (bottom). The arrows indicate injection. The excess injection head is 20 m.

In order to verify the solutions obtained with the numerical flow model, flow rates and hydraulic heads are calculated for three reference cases denoted A, B, and C, see Table 1. The evaluation of the hydraulic properties of the flow fields simulated is made with both Jacob-Lohman's graphical solution technique (Jacob and Lohman, 1952) and Moye's formula. Figure 9 shows the graphical solution technique and Figure 10 shows a plot of the data in Table 1. Jacob-Lohman's formulae for calculating the transmissivity T_j and the storativity S_j from the straight line can be written as

$$T_j = \frac{0.183}{H\ \Delta(1/Q(t))} \tag{7a}$$

$$S_j = \frac{T_j}{r_w^2}\, 10^{\left(2.13 - \frac{(1/Q(t))_{1\ \mathrm{min}}}{\Delta(1/Q(t))}\right)} \tag{7b}$$

where $\Delta(1/Q(t))$ is the change in flow rate during a log_{10} logarithmic time cycle and $1/Q(t)_{1\ \mathrm{min}}$ is obtained by extrapolating the straight line to 1 minute. (The graphical technique and formulae used (Cooper and Jacob, 1946) for interpreting the recovery period (see, e.g., Nilsson, 1989, 1990) are about the same as those of Jacob-Lohman.)

As shown in Figure 9 the duration of the injection period simulated is 15 minutes, which equals the period of time used in conjunction with 3 m packer tests within the Swedish nuclear waste repository programme. Andersson *et al.* (1988) report that occasionally the test period can be prolonged up to 120 minutes. In a real field test situation, it is generally impossible to maintain a constant injection head during the first 10 to 100 seconds from the onset due to technical constraints, which means that the flow rates recorded during this period of time are not reliable for interpretation. Therefore, whenever a transient interpretation is desired using Jacob-Lohman's straight-line approximation, the straight line is fitted to the data recorded just before the injection test is shut-in (personal communications with Mr. Jan-Erik Andersson, GEOSIGMA, 1992).

According to theory equations (7a) and (7b) give reliable values of T and S provided that there is no borehole skin and that the dimensionless time $t_D = (Tt)/(Sr_w^2)$ is greater than 1,000. For the three reference cases - A, B, and C - $t_D \geq 1{,}000$ while $t \geq 12.5$, 0.58, and 0.03 minutes, respectively, and Jacob-Lohman's straight-line approximation is readily adapted to the flow rates simulated. As shown in Table 1 and Figure 10, the values of T and S calculated with Jacob-Lohman's equations compare well with the reference values. Thus, the implementation of the numerical flow model is considered to be verified.

Tab. 1 Comparison between the results calculated with Jacob-Lohman's (T_j and S_j) and Moye's (T_m) formulae. The reference values used (T_{ref} and S_{ref}) are called case A, B, and C, respectively.

CASE	T_{ref} (m^2/s)	S_{ref} (-)	T_j (m^2/s)	S_j (-)	T_m (m^2/s)
A	1.00E-9	9.56E-7	9.62E-10	8.22E-7	1.20E-9
B	1.00E-7	4.43E-6	9.19E-8	5.19E-6	8.52E-8
C	1.00E-5	2.06E-5	9.06E-6	2.79E-5	6.57E-6

Although the flow rate is gradually decreasing with time while transient conditions are prevailing, it is generally assumed in geological and civil engineering that the interpretation can be made with a steady-state formula such as Moye's formula. Doe and Remer (1981) compared steady-state flow and transient flow analyses. They concluded that the error in assuming a steady-state flow is less than one order of magnitude for reasonable values of the storativity. As shown in Table 1 and in Figure 10, Moye's formula gives values of the transmissivity that compare well with the three values interpreted with Jacob-Lohman's formula.

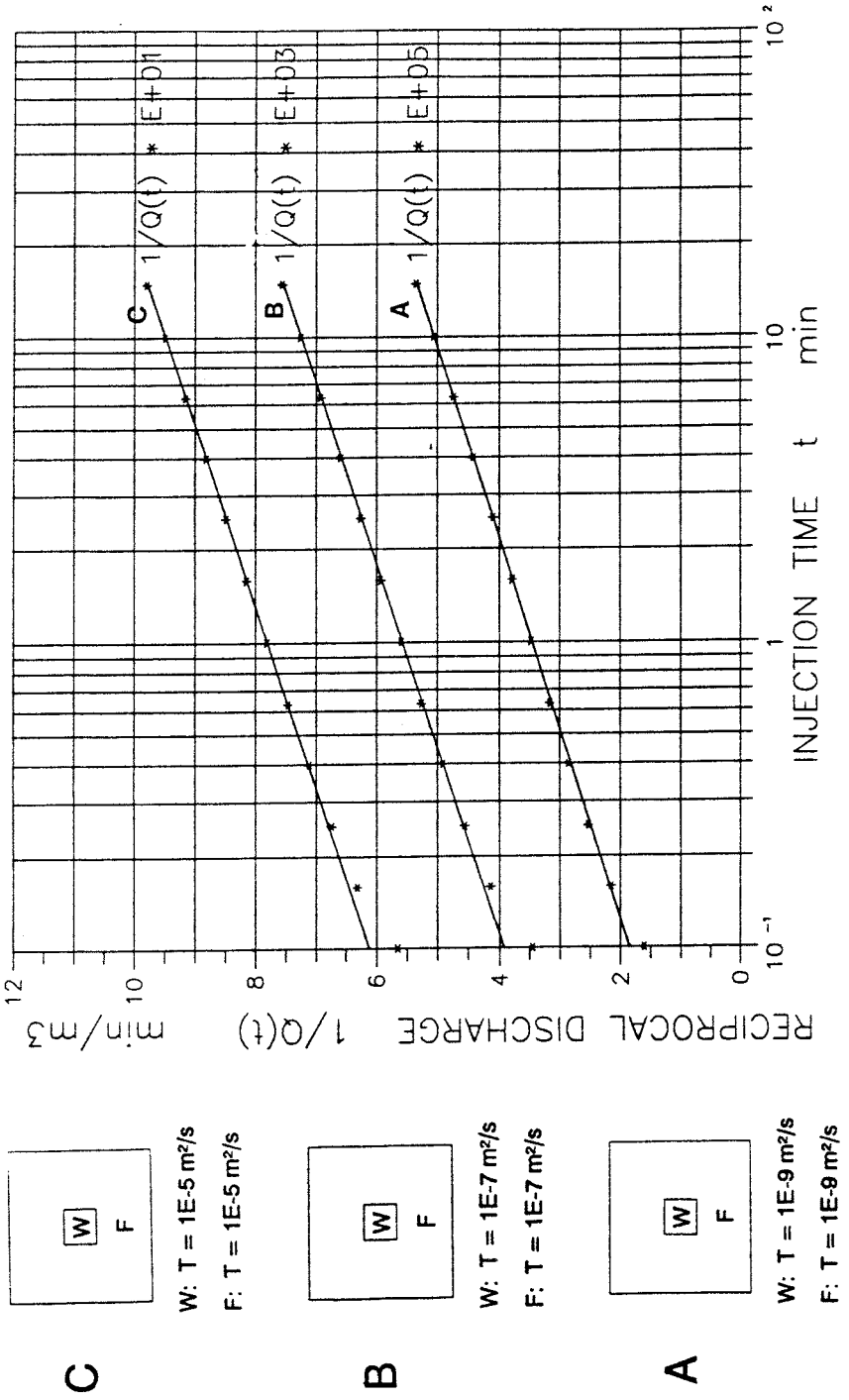

Fig. 9 Semi-logarithmic plots of $1/Q$ vs. t for the three reference cases studied, see Table 1. The figure shows Jacob-Lohman's graphical solution technique - the straight-line approximation. T_W and T_F denote the transmissivities of the borehole block and the surrounding formation blocks, respectively.

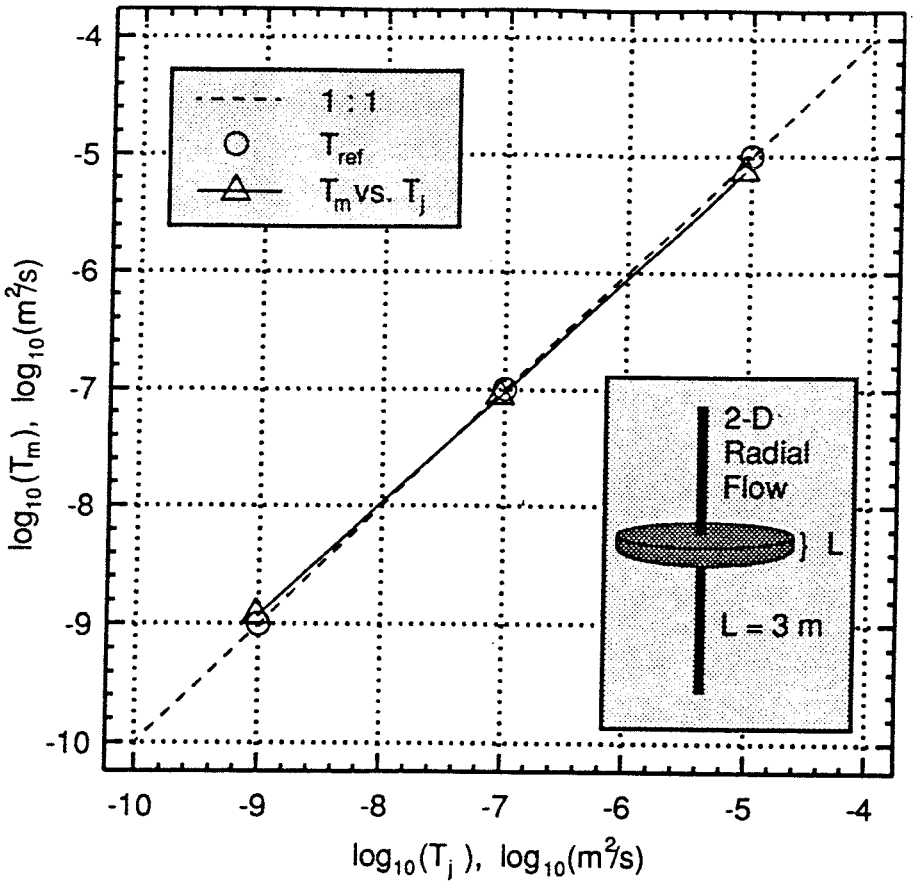

Fig. 10 Comparison between the results calculated with Jacob-Lohman's (T_j) and Moye's (T_m) formulae in relation to the three reference values used, see Table 1.

Although we may consider that the numerical flow model is verified and that the results compare well, it is important to note that a good agreement between the two formulae used is not evident. For instance, the small discrepancies observed in Figure 10 would have been different for a three-dimensional flow domain (cf. Figure 5). The inset in the lower left corner of Figure 10 indicates that the flow domain in this study is radial and that the test section length is L = 3 m. For a test section length of L =30 m, the values of T_m in Table 1 increase by 50%, whereas the values of T_j are unaffected. Moreover, for a transient test the volumetric flow rate decreases with time, i.e., the duration of the test period affects the value of T_m but not T_j. By way of conclusion, the good agreement obtained in this study is to some extent explained by the chosen values of the dimensionality of the flow domain, the test section length, and the duration of the test period. However, the data used for the model set-up in are in accordance to real specifications including the implicit assumptions made while using Moye's and Jacob-Lohman's formula for interpretation.

Doe and Remer (1981) concluded further that the success of applying a steady-state flow formula to some extent depend on the assumed value of the radius of influence. For instance, in Moye's formula the radius of influence is replaced by the length of the test section. Thus, the geometric factor is in this case devoid of any notion about the radius of influence, which leads to an uncertainty about the volume of rock affected. However, in Thiem's formula (Thiem, 1906), which is the equation used by Doe and Remer (1981), the radius of influence is maintained

$$T = \frac{Q}{2\pi H} ln(r_e / r_w) \tag{8}$$

where r_e is the radius of influence, which in this case corresponds to the radius to an outer constant-head boundary. Following Doe and Remer (1981), we may substitute the flow rate in equation (8) by the average flow rate injected during the simulation period in order to calculate an estimate of r_e. For reference case B, see Table 1, the calculations yield that $r_e \approx 5.3$ m after 15 minutes and that $r_e \approx 15$ m after 120 minutes of injection. For the purpose of this study, we may compare these values with the values computed with Cooper-Jacob's expression of the radius of influence valid for a constant flow rate test (Cooper and Jacob, 1946; Jacob, 1950)

$$r_e = \sqrt{\frac{2.25\,T\,t}{S}} \tag{9}$$

It is interesting to note that this expression is devoid of any notion about the flow rate. For reference case B equation (9) yields that $r_e \approx 6.8$ m after 15 minutes of injection and that $r_e \approx 20$ m after 120 minutes of injection. Figure 11 shows the numerical solution of the hydraulic head for reference case B after 15 and 120 minutes of injection, respectively. The contoured heads are chosen in a logarithmic fashion between H and $0.001H$ where H is the excess injection head, which in this study is set to 20 m. The two plots show that the numerically calculated radius of influence in each case is larger than the previous values using the assumptions and formulae described above. After 15 minutes of injection the $0.001H$ contour (0.02m) is at about 12 m, whereas after 120 minutes of injection it is at about 33 m. The head values of the nodes on the outer boundary of the numerical flow domain are unaffected. We recall that the plots in Figure 11 correspond to a homogeneous porous medium. The impact of heterogeneity has an unknown effect as yet, although one may expect that the hydraulic conditions closest to the borehole are very important.

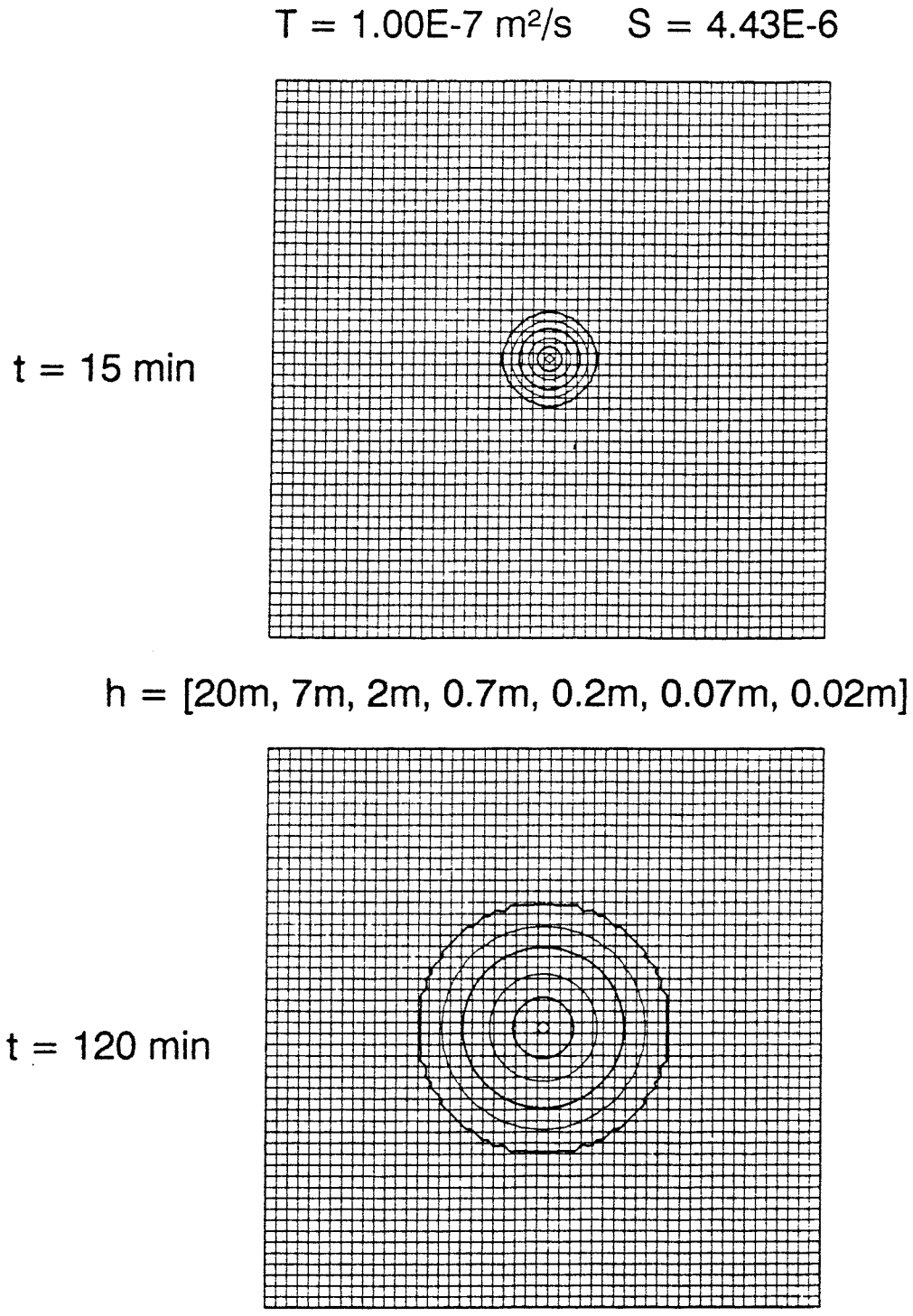

Fig. 11 Numerical calculated radii of influence for reference case B after 15 and 120 minutes of injection, respectively. The size of each grid block is $(3m)^2$.

Chapter 4

Experimental set-up

The Monte Carlo method (see, e.g., Peck *et al.*, 1988; Freeze *et al.*, 1990) is a powerful alternative to deterministic numerical modelling of flow and mass transport in a heterogeneous medium. Rather than depending on the detailed information about the actual field conditions or a number of debatable assumptions, as required by a deterministic model, the modelling is carried out under uncertainty. The turning bands method (Mantoglou and Wilson, 1982) is used in this study for generating unconditional realisations of correlated transmissivities, whereas an ordinary random number generator (Schrage, 1969) is used for generating unconditional realisations of non-correlated transmissivities.

Besides studying the sensitivity to the statistical structure of the transmissivity field, the sensitivity to the transmissivity value closest to the borehole is also studied. The idea of a borehole giving direct access to virgin unaltered rock is practically a theoretical concept. In reality, it is important to recognise that the hydraulic properties of the rock in the immediate vicinity of the borehole are easily altered by the drilling process. Following the petroleum terminology, this is envisaged as a "skin" and its effect on flow into or out of the borehole is termed skin effect (see, e.g., Earlougher, 1977). Mathematically, the skin factor ξ can have different signs. The sign convention adopted is that a zone of reduced transmissivity results in a positive skin factor and vice versa. For deep boreholes in fractured hard rocks a negative skin effect is likely to occur due to hydraulic fracturing in conjunction with the core drilling. However, the possibility for a positive skin effect due to mechanical clogging by the drilling debris should not be neglected. By way of conclusion, the transmissivity value in the immediate vicinity of the borehole is not necessarily correlated with the transmissivity field of the surrounding formation.

The input data to the two random number generators used for generating the transmissivity values to the grid blocks of the numerical flow model are based on statistical analyses of 10 -15 minutes long constant-head injection tests made with a double-packer spacing of 3 m. The transmissivity values used in this study to derive a characteristic mean, variance, and covariance function are interpreted with Moye's formula and come from field tests made at the Finnsjön study site and the Äspö Hard Rock Laboratory (see, e.g., Nilsson, 1989, 1990; Gustafson *et al.*, 1989; Cvetkovic and Kung, 1989; Liedholm,

1991a,b). The input data derived compare well with the hydraulic conditions at the Swedish study sites in fractured hard rocks in general (for a statistical overview, see Winberg, 1989).

Based on a large number of observations made in different types of rocks it is generally concluded that transmissivity data obey a log-normal frequency distribution (cf. Freeze, 1975). A relevant example for the conditions encountered in Swedish hard rocks is shown in Figure 4, which supports this conclusion. In this study, a median transmissivity value of $T_F = 10^{-7}$ m^2/s and a log-normal standard deviation of $\sigma_Y = 4$, where $Y = ln(T)$, are used for generating the block transmissivities of the heterogeneous formation surrounding the borehole in each realisation. The generated transmissivity value in the vicinity of the borehole in each realisation is replaced by a prescribed value representing an alteration due to, conceptually at least, hydraulic fracturing, mechanical clogging, or any other relevant process that may cause a positive or negative skin effect. The technique used is shown in Figure 12 and should not be confused with conditional simulation, which is a totally different concept (see, e.g., Delhomme, 1979; Dagan, 1982).

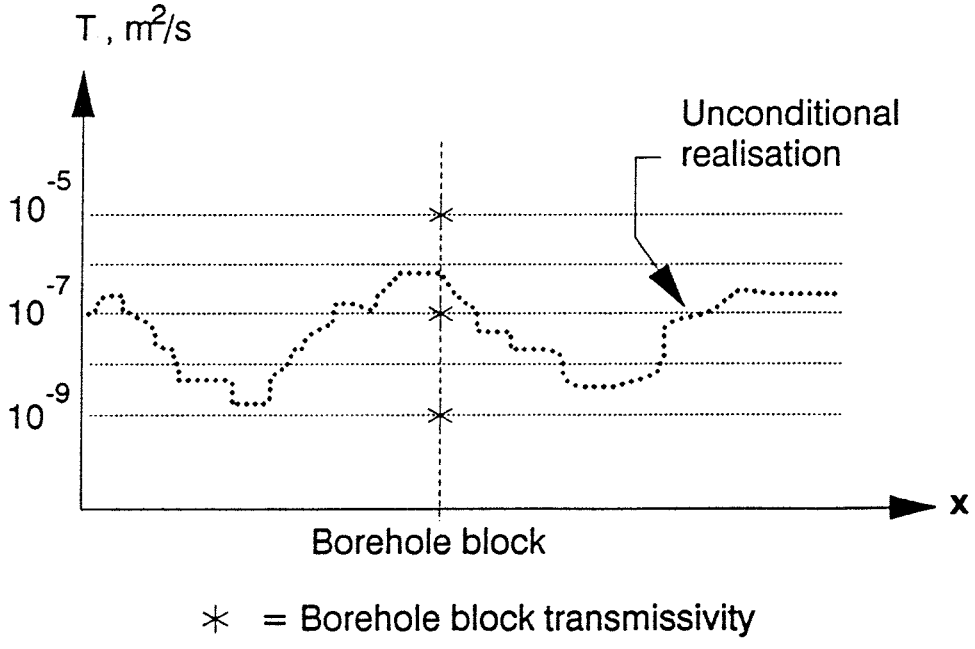

Fig. 12 Illustration of the technique used to obtain a prescribed transmissivity value of the borehole. block.

Black and Barker (1987) concluded in their overview of various interpretation errors in conjunction with different single-borehole tests, that a steady-state interpretation of the transmissivity (e,g,, Moye's formula) is distorted by skin effects, whereas a transient interpretation (e.g., Jacob-Lohman's or Cooper-Jacobs's formulae) is unaffected. Figure 13 shows a comparison between interpretations made with Moye's and Cooper-Jacob's formulae for one of the boreholes at the Äspö Hard Rock Laboratory (cf. Figure 3). (We recall that the graphical technique and formulae of Cooper-Jacob compare well with those of Jacob-Lohman, see Chapter 3.)

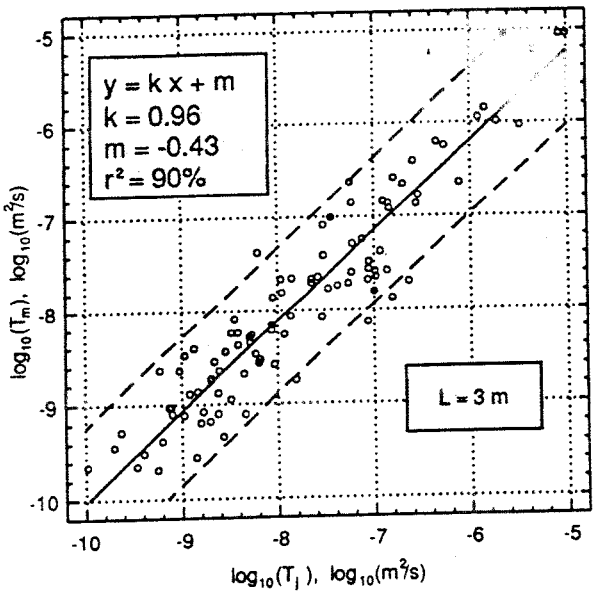

Fig. 13 Comparison between interpretations made with Moye's (T_m) and Jacob-Lohman's (T_j) formulae. Borehole KAS03 at Äspö Hard Rock Laboratory. L = 3 m and t = 10 minutes.

The regression line in Figure 13 has a slope close to unity and an intercept close to zero. Hence, for this particular borehole there is no systematic difference between steady-state and transient interpretations (cf. Doe and Remer, 1981). Locally, however, the differences can be quite large. For example, the 95% confidence interval for new predictions covers roughly two orders of magnitude, i.e., $T_m^{95\%} \approx 10^{\pm 1}\, T_c$, where T_m and T_c denote the transmissivities of Moye and Cooper-Jacob, respectively. In Chapter 3, we concluded that Moye's and Jacobs-Lohman's formulae compare well for a 15 minutes long constant-head injection test with a double-packer spacing of 3 m in a two-dimensional homogeneous formation without borehole skin. Provided that these constraints apply to the data plotted in Figure 13 and that the conclusion of Black and Barker (1987) is correct, the scattering of the data could be seen as a tentative plot of the skin factor.

The experimental set-up used in this study consists of two parts with three cases each, which can be described as follows:

Part 1 (cases D-F)

For a prescribed transmissivity value of the borehole block of $T_W = 10^{-7}$ m^2/s, three values of the correlation range R_Y are studied, namely 3 m, 18 m, and 36 m.

Part 2 (cases G-I)

For a given input value of the correlation range of $R_Y = 18$ m, three transmissivity values of the borehole block T_W are studied, namely 10^{-9} m^2/s, 10^{-7} m^2/s, and 10^{-5} m^2/s.

The shortest range (3 m) equals the side length of a grid block, see Figures 1 and 6. That is to say, although the ordinary number generator generates non-correlated block transmissivities there is a perfect correlation (homogeneity) within a block due to the discretisation. The longer ranges (18 m and 36 m) are generated with the turning bands method using an isotropic and exponential covariance model C (see, e.g., de Marsily, 1986)

$$C(h) = \sigma_Y^2 \, exp\left(-\frac{h}{\lambda_Y}\right) \tag{10}$$

where h is the separation distance and λ_Y is a correlation parameter defined as the distance where the two-point correlation is reduced by a factor e. For such a model the correlation range R_Y is about 3 λ_Y. For each combination of T_W and R_Y 200 realisations are generated. The different combinations (or cases) are shown in Table 2. The transient flow problem is simulated for each realisation using the numerical flow model described above, and the transmissivities are interpreted with Moye's formula.

Tab. 2 Each case D-I is studied by 200 realisations. The realisations in case D are generated with an ordinary random number generator, whereas the realisations in cases E-I are generated with the turning bands method using an isotropic and exponential variogram model. For the purly random case D, $R_Y \approx \Delta x = \Delta y = 3$ m, and for the correlation cases E-I, $R_Y \approx 3\ \lambda_Y$.

T_W (m^2/s)	λ_Y (m)	R_Y (m)	T_W (m^2/s)	λ_Y (m)	R_Y (m)
D: 10^{-7}	-	3	**G:** 10^{-9}	6	18
E: 10^{-7}	6	18	**H:** 10^{-7}	6	18
F: 10^{-7}	12	36	**I:** 10^{-5}	6	18

As mentioned above, the input data to the two random number generators used for generating the transmissivity values to the numerical flow model are based on statistical analyses of transmissivity measurements made with a double-packer spacing of 3 m. Thus, the conceptual thickness of the two-dimensional horizontal slab is 3 m as well (cf. Figure 1) although the thickness of the slab as such is unimportant for the mathematical formulation of the problem. However, using input data derived from statistical analyses of an essential vertically orientated piece of information, i.e., measurements in vertical and sub-vertical boreholes, for generating a heterogeneous medium in a horizontal plane, implies that we indirectly assume that the statistical structures reported in the literature are statistically isotropic. The latter assumption cannot be verified in general due to lack of data. According to Winberg (1991), a geostatistical analysis of transmissivity data from boreholes of varying orientation in the Stripa mine, indicates a statistically isotropic covariance structure.

We consider it important to stress that a consistent geostatistical analysis of borehole transmissivity data implies that: (*i*) the transmissivities have a constant support scale, e.g., a constant radius of influence, and (*ii*) transmissivity heterogeneities in the region below and above each test section have no significant influence on the transmissivity of the tested section between the packers. However, none of these conditions is evident. In particular, the assumption about a constant support scale is debatable.

Besides the transmissivity field, the storativity field is also considered to be heterogeneous in the present study. Rock compressibility data given by de Marsily (1986) are used in combination with an empirical relationship between the hydraulic conductivity K and the effective porosity ϕ of the rock mass of Swedish hard rocks suggested by Winberg *et al.* (1990) who refer to data reported by Carlsson and Olsson (1981)

$$ln(\phi) = 0.34\ ln(K) \tag{11}$$

The resulting positive $\sqrt[3]{}$ relationship between the log-storativity and the log-transmissivity fields is shown in Figure 14. By way of conclusion, the random variable in this study is not the transmissivity but the diffusivity T/S. Field observations of the storativity in fractured hard rocks are very sparse, but the $\sqrt[3]{}$ relationship between S and T shown in Figure 14 is considered to be relevant for the conditions at the Finnsjön study site (personal communications with Mr. Jan-Erik Andersson, GEOSIGMA, 1992).

Following equation (9), r_e is proportional to $\sqrt{(T/S)}$. For a $\sqrt[3]{}$ relationship between S and T we may therefore expect, at least as a working hypothesis, that $r_e \propto \sqrt[3]{T}$. If a relation-

ship of this order is assumed to be appropriate for the natural conditions in fractured hard rocks, r_e will vary with two orders of magnitude when T varies six orders of magnitude. According to the transmissivity data shown in Figure 3, such a range in T is not irrelevant. Consequently, the doubts raised in this study about a spatially varying support scale in conjunction with conventional double-packer tests are considered to be justified.

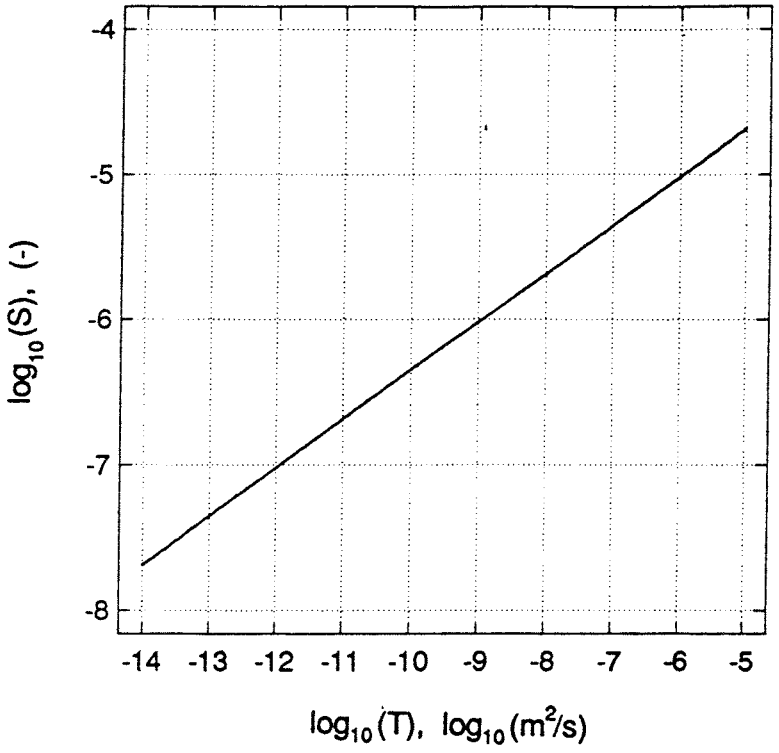

Fig. 14 Assumed relationship between the storativity and the transmissivity fields.

Chapter 5

Data interpretation

The interpretation of the numerical simulations is automated. However, it is necessary to show and discuss a few figures that illustrate the intermediate steps of the data analysis before presenting the results. Figure 15 shows an example of one of the realisations studied, which in this particular case is generated with the turning bands method using an isotropic and exponential correlation with $T_G = 10^{-7}$ m^2/s, $\sigma_Y = 4$, and $R_Y \approx 18$ m. The variability of the transmissivity field in Figure 15 is divided into eight percentiles, where light colours represent transmissive blocks and vice versa. The heterogeneous medium has median transmissivity of $T_F = 2.15 \cdot 10^{-7}$ m^2/s.

The realisation in Figure 15 is used as input to the numerical flow model three times with different values of the borehole block transmissivity corresponding to cases G-I in Table 2, i.e., $T_W = 10^{-9}$, 10^{-7}, or 10^{-5} m^2/s, respectively. Figure 16 shows the hydraulic head solutions after 15 minutes of injection. For the purpose of this study we define the radius of influence r_e at $t = 15$ minutes to be equal to the radius of the head contour $h = 0.02$ m. Figure 16 shows that the value of T_W has a crucial impact on r_e and that the envelope of r_e varies with orientation. The irregularity of the envelope is in this study characterised by $r_{e,min}$ and $r_{e,max}$, which define its minimum and maximum values, and by $r_{e,ave}$ and $r_{e,std}$, which define its mean and the standard deviation, respectively, see Figure 17.

In Figure 18, the reciprocal value of the volumetric flow rate is plotted versus time. In the upper plot $T_W = 10^{-9}$ m^2/s, in the middle plot $T_W = 10^{-7}$ m^2/s, and in the lower plot $T_W = 10^{-5}$ m^2/s. The different graphs drawn in each plot correspond to the situations shown in the insets to the left of the plot. The insets denoted #1 correspond to cases A-C in Table 1, i.e., a homogeneous formation with $T_W = T_F = 10^{-9}$, 10^{-7}, or 10^{-5} m^2/s, respectively. The insets denoted #2 correspond to cases G-I in Table 2, i.e., a heterogeneous formation with $T_W = 10^{-9}$, 10^{-7}, or 10^{-5} m^2/s, respectively. In Figure 18, $T_F = 2.15 \cdot 10^{-7}$ m^2/s corresponding to the realisation shown in Figure 15. The insets denoted #3 correspond to a homogeneous formation with $T_F = 10^{-7}$ m^2/s, where the borehole block transmissivity is either affected by a positive skin ($T_W = 10^{-9}$ m^2/s) or by a negative skin ($T_W = 10^{-5}$ m^2/s). The lower plot in Figure 18 is shown in Figure 19 and discussed in detail below.

From the upper plot in Figure 18 we conclude that for a 15 minutes long constant-head injection test it is practically impossible to separate the three situations studied regardless of the interpretation method used. That is to say, for a borehole block transmissivity of $T_W = 10^{-9}$ m^2/s (or less) we cannot determine whether the surrounding formation is homogeneous or heterogeneous. If the test section between the packers is of low transmissivity due to reasons that cause a positive skin, the conditions close to the borehole may be severely altered and no longer represent the actual conditions of the surrounding formation. Thus, a positive skin will drastically distort fracture network transmissivity calibrations as well as geostatistical analyses and conditional simulations.

For a borehole block transmissivity of $T_W = 10^{-7}$ m^2/s (see the middle plot in Figure 18) the possibilities for a detailed analysis are slightly improved, whereas the best possibilities occur for a borehole block transmissivity of $T_W = 10^{-5}$ m^2/s (see the lower plot in Figure 18). Applying Moye's and Jacob-Lohman's formulae to the three graphs plotted in Figure 19 we get the following results:

Graph/inset #3 ($T_W = 10^{-5}$ m^2/s, $T_F = 10^{-7}$ m^2/s):
$T_m = 3.18 \cdot 10^{-7}$ m^2/s, $T_j = 1.11 \cdot 10^{-7}$ m^2/s

Graph/inset #2 ($T_W = 10^{-5}$ m^2/s, $T_F = 2.15 \cdot 10^{-7}$ m^2/s):
$T_m = 8.52 \cdot 10^{-7}$ m^2/s, $T_j = 6.10 \cdot 10^{-7}$ m^2/s

Graph/inset #1 ($T_W = T_F = 10^{-5}$ m^2/s):
$T_m = 6.57 \cdot 10^{-6}$ m^2/s, $T_j = 9.06 \cdot 10^{-6}$ m^2/s

If we compare the upper and middle graphs with the lower graph, we conclude that the conditions of the borehole block cease to prevail already after a few tens of a minute. Thus, in either case both formulae compare well and reflect the transmissivity of the surrounding formation rather than the transmissivity of the borehole block Further, by comparing the results of graph/inset #3 with the results of case B in Table 1, i.e.,

Graph/inset #3 ($T_W = 10^{-5}$ m^2/s, $T_F = 10^{-7}$ m^2/s):
$T_m = 3.18 \cdot 10^{-7}$ m^2/s, $T_j = 1.11 \cdot 10^{-7}$ m^2/s

Case B in Table 1 ($T_W = 10^{-7}$ m^2/s, $T_F = 10^{-7}$ m^2/s):
$T_m = 8.52 \cdot 10^{-8}$ m^2/s, $T_j = 9.19 \cdot 10^{-8}$ m^2/s

we may infer a few things concerning the numerical flow model and the skin effect. Firstly, the differences between T_j and T_F reflect to some extent imperfections of the numerical flow model but also the uncertainty of fitting a straight line to a data set. Secondly, the value of T_m for graph/inset #3 is affected by a negative skin even if is almost negligible. The definition of borehole skin can be written as (cf. Earlougher, 1977)

$$\xi = \left(\frac{T_F}{T_\xi} - 1 \right) ln \left(\frac{r_\xi}{r_w} \right) \qquad (12)$$

where T_ξ and r_ξ are the transmissivity and the radius of a symmetric zone affected by skin, respectively. For graph/inset #3, $T_\xi = T_W = 10^{-5}$ m^2/s and $r_\xi \approx \Delta x/2 = 1.5$ m. Using these values in equation (12) yields that $\xi \approx -3.94$. Using $r_w = r_\xi \approx 1.5$ m in equation (5), changes Moye's transmissivity from $3.18 \cdot 10^{-7}$ m^2/s to $6.65 \cdot 10^{-8}$ m^2/s, which compares well with the unaltered transmissivity value determined in case B, i.e., $8.52 \cdot 10^{-8}$ m^2/s.

The plots in Figures 16 and 18 clearly demonstrate the sensitivity to the hydraulic conditions in the vicinity of the borehole. As mentioned previously, Black and Barker (1987) concluded that an interpretation of the rock transmissivity using Moye's formula is distorted by skin effects, whereas an interpretation using Jacob-Lohman's formula is unaffected. However, considering the small differences in the interpretations obtained above in relation to Figures 18 and 19, the conclusion made in this study is that Moye's and Jacob-Lohman's formulae approximately render the same results regardless of the value of the borehole block transmissivity. The practical implication of this conclusion is interesting. For instance, Figure 12 shows a comparison between interpretations made with Moye's and Jacob-Lohman's formulae for a number of real double-packer tests made in one of the boreholes at the Äspö Hard Rock Laboratory. It is not reasonable that a varying skin effect is the only cause to the scattering of the data plotted in Figure 12 considering the result that the difference between the two formulae is small regardless of the value of the borehole block transmissivity.

The good agreement between Moye's and Jacob-Lohman's formulae is of course limited by the conditions studied here, namely a 15 minutes long constant-head injection test in a perfectly two-dimensional flow domain with an essentially radial flow regime. What are the flow conditions for real double-packer tests in natural rocks? Braester and Thunvik (1982, 1984) concluded theoretically that for short test section lengths, the flow regime around a borehole deviates from being radial to become somewhat more spherical. Jacob-Lohman's formulae assumes a perfectly radial flow regime, whereas Moye's formulae is more adaptive to a radial-spherical flow regime (see Figure 5). Thus, for non-radial flow regimes, results computed with Moye's and Jacob-Lohman's formulae do not necessarily compare.

Following Barker (1988), the flow around the borehole may take any dimension including fractional dimensions, see Figure 2. Geier and Doe (1992) compared interpretations made with Moye's formula with interpretations made with the fractional dimension theory

for a number of double-packer test data from the Finnsjön study area. They concluded that the two methods compare well in many cases but that significant deviations can occur in situations where the flow dimension is close to unity, e.g., a situation where an impervious rock mass is intersected by a single channel of high conductivity. By way of conclusion, the results obtained in this study together with the results of Braester and Thunvik (1982, 1984), Barker (1988), and Geier and Doe (1992) suggest that the scattering of the data plotted in Figure 12 could be due to, besides skin effects, (*i*) interpretation errors, and/or (*ii*) non-radial flow regimes around the tested sections.

In Figure 20 the effects of a hypothetical diagonal fracture zone on the radius of influence are shown. The purpose of this figure is to stimulate the imagination of how fractional dimensions of flow may arise due to site specific conditions of heterogeneity. The formation the upper plot in Figure 20 is homogeneous with $T_F = 10^{-7}$ m^2/s except for a diagonal fracture zone (running from the upper left to the lower right corner), which has a transmissivity of $T_Z = 10^{-5}$ m^2/s. In the lower plot in Figure 20, the formation is identical to that in shown Figure 15 except for the diagonal fracture zone. Thus, the lower plot in Figure 20 should be compared with the lower plot in Figure 16.

Fig. 15 Example of one of the realisations studied. Note the borehole block in the centre. The realisation is used as input to the numerical flow model three times with different values of the borehole block transmissivity corresponding to cases G-I in Table 2.

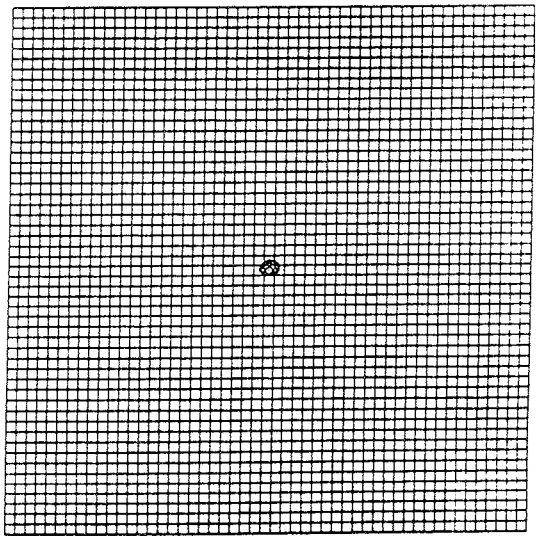

$T_W = 10^{-9}\ m^2/s$

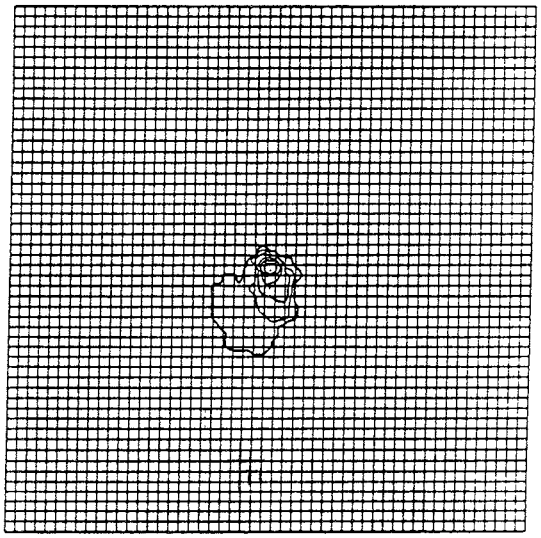

$T_W = 10^{-7}\ m^2/s$

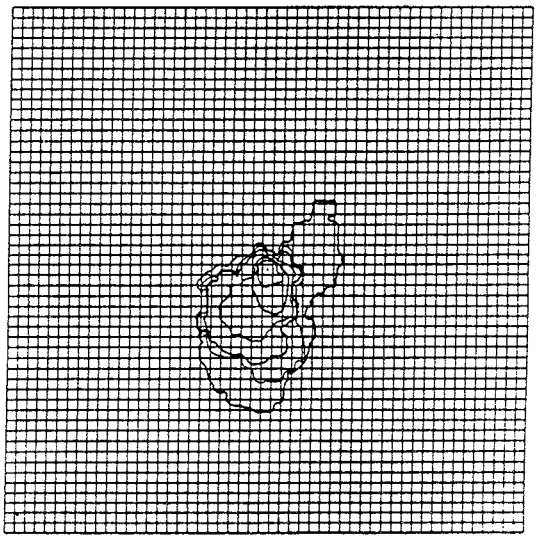

$T_W = 10^{-5}\ m^2/s$

Fig. 16 Hydraulic head contours after 15 minutes of injection for the realisation shown i Figure 15. The upper contour plot refers to case G, the middle plot to case H, and the lower plot to case I, see Table 2. The head contours shown correspond to h = {20, 7, 2, 0.7, 0.2, 0.07, 0.02} m.

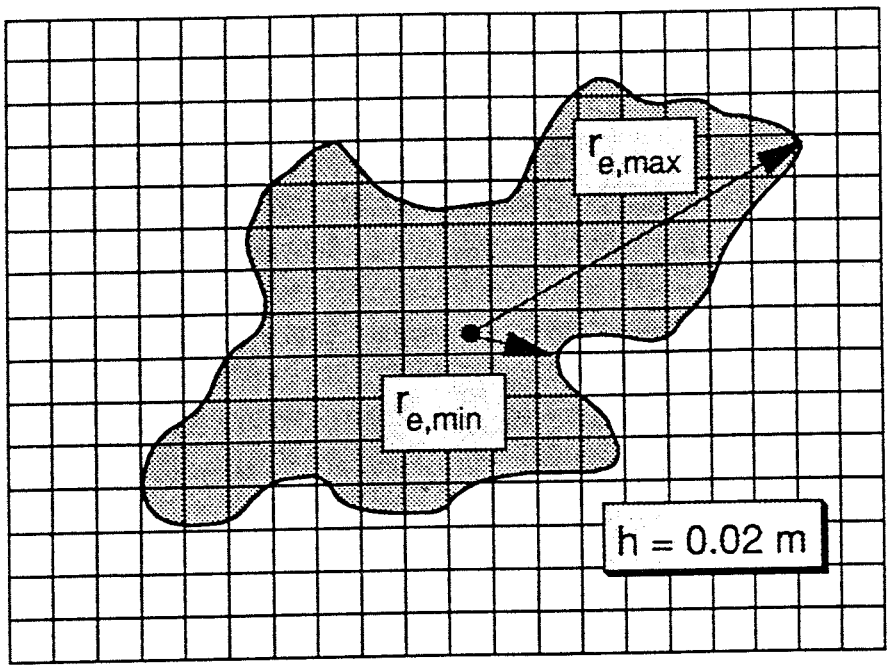

● = Borehole

$$r_{e,ave} = \frac{1}{n_{2\pi}} \sum_{i=0}^{2\pi} (r_e)_i$$

$$r_{e,std} = \sqrt{\frac{1}{(n_{2\pi} - 1)} \left(\sum_{i=0}^{2\pi} (r_e)_i^2 - n_{2\pi} (r_{e,ave})^2 \right)}$$

$$\langle r_{e,ave} \rangle = \frac{1}{200} \sum_{i=1}^{200} (r_{e,ave})_i$$

Fig. 17 The definitions of r_e, $r_{e,min}$, $r_{e,max}$, $r_{e,ave}$, and $r_{e,std}$ refer to the position and the irregularity of the head contour h = 0.02 m after 15 minutes of injection.

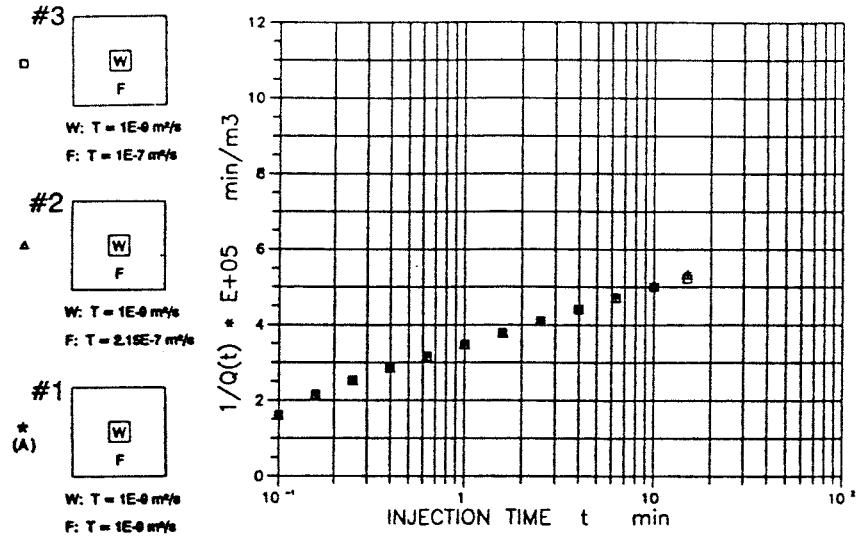

$T_W = 10^{-9}\ m^2/s$

$T_W = 10^{-7}\ m^2/s$

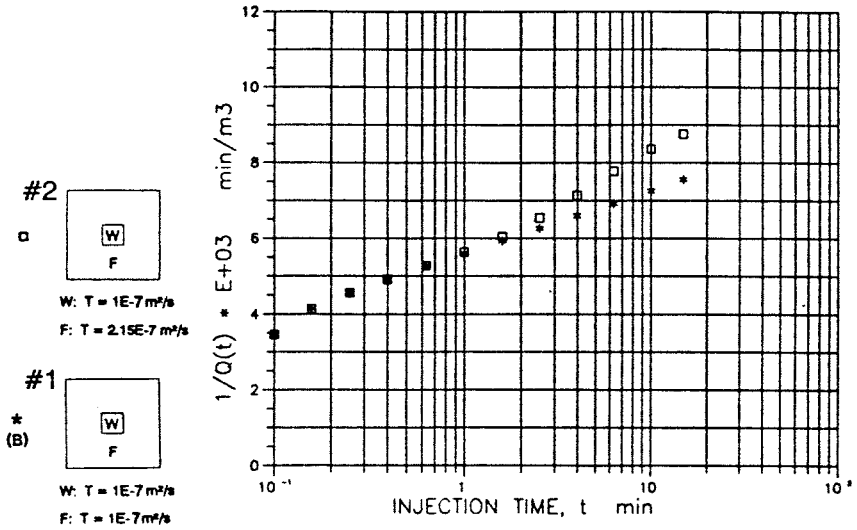

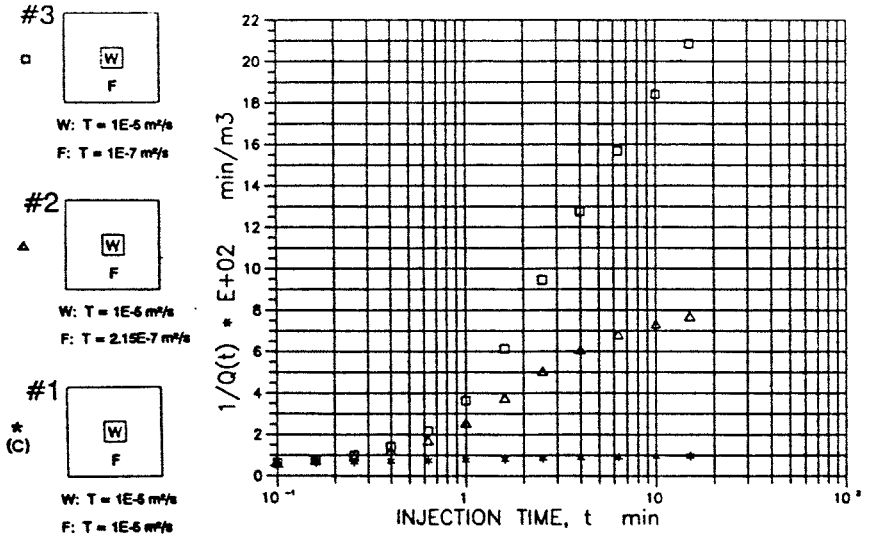

$T_W = 10^{-5}\ m^2/s$

Fig. 18 Plots of $1/Q$ vs. $log_{10}(t)$. The insets to the left of each plot show the flow situations studied. T_W and T_F are the transmissivities of the borehole block and the surrounding formation, respectively.

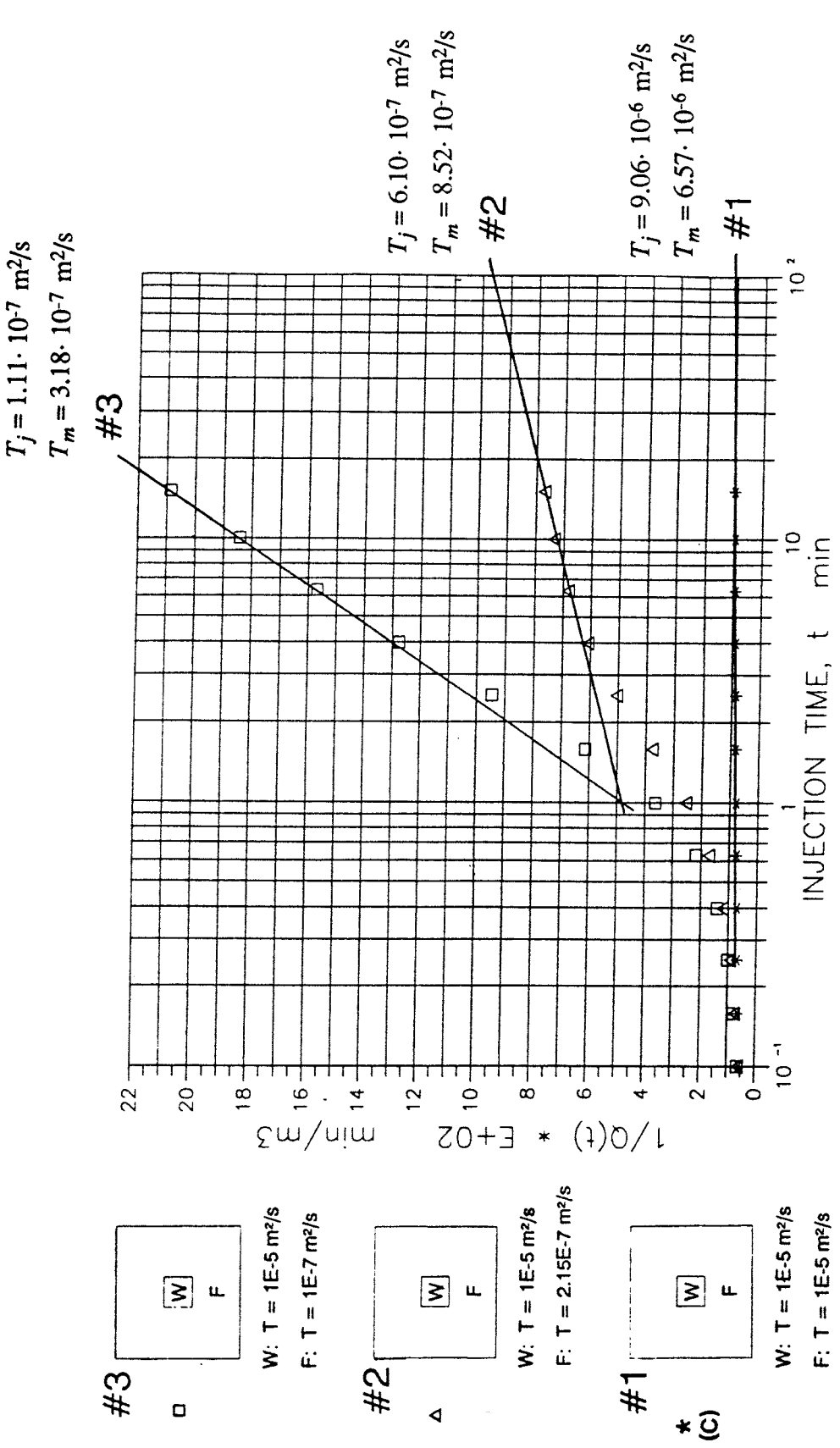

Fig. 19 Plot of $1/Q$ vs. $log_{10}(t)$ (cf. the lower plot in Figure 18). The insets to the left of the plot show the flow situations studied. T_W and T_F denote the transmissivities of the borehole block and the surrounding formation, respectively. T_m and T_j denote the transmissivities interpreted with Moye's and Jacob-Lohman's formulae, respectively.

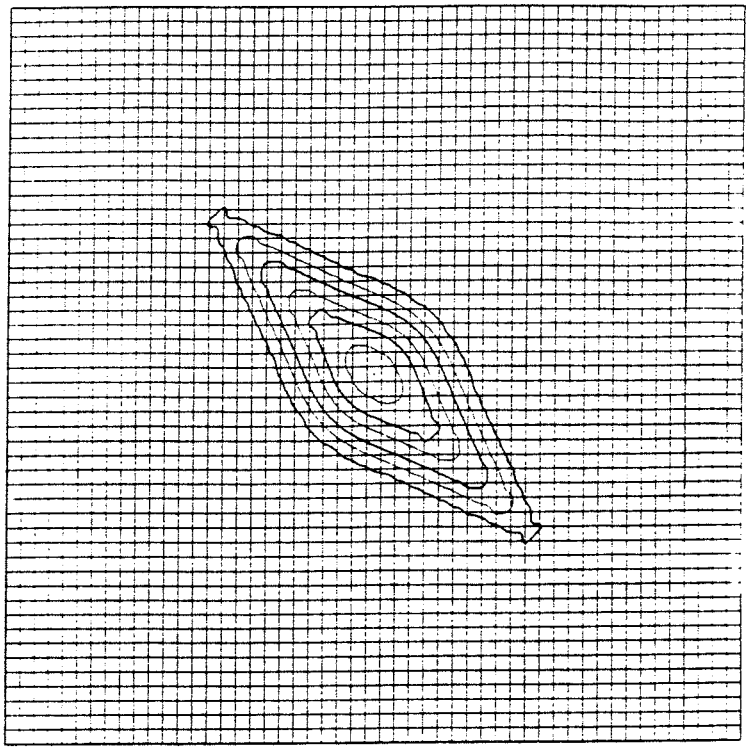

$T_W = T_Z = 10^{-5}\ m^2/s$

$T_F = 10^{-7}\ m^2/s$

Fracture in homogeneous rock

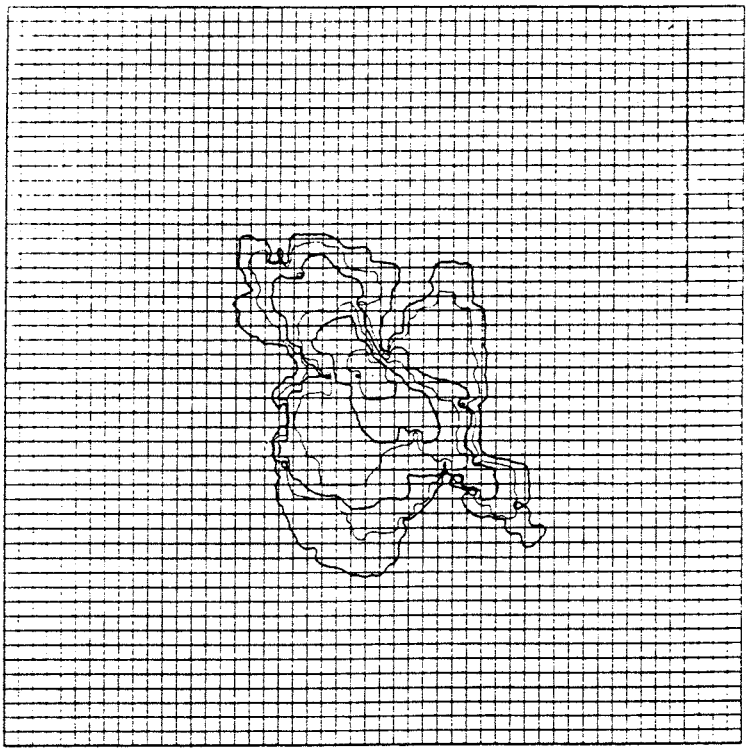

$T_W = T_Z = 10^{-5}\ m^2/s$

$T_F = 2.15 \cdot 10^{-7}\ m^2/s$
(median)

Fracture in heterogeneous rock

Fig. 20 Hydraulic head contours after 15 minutes of injection in a homogeneous (top) and a heterogeneous formation (bottom), each intersected by a diagonal fracture zone. The heterogeneous formation is identical to the realisation shown in Figure 15, except for the diagonal fracture zone. The head contours shown correspond to h = {20, 7, 2, 0.7, 0.2, 0.07, 0.02} m.

Chapter 6

Monte Carlo results

The Monte Carlo method is used in this study to investigate (*i*) the sensitivity of T_m and $r_{e,ave}$ to different statistical structures (R_Y), see cases D-F in Table 2, and (*ii*) the relationship between T_m and $r_{e,ave}$ for a given statistical structure, see cases G-I in Table 2. A multinormal distribution is assumed for the transmissivity fields generated with a linear relationship between $log_{10}(T)$ and $log_{10}(S)$, see Figure 14. The results are shown in Table 3 and in Figures 21-25.

Table 3 shows that the different ensemble mean values of T_m and $r_{e,ave}$ compare well with each other, respectively, and that they also compare well with the values of T_m and r_e for the corresponding homogeneous case B (cf. Table 1).

Tab. 3 Case B is a homogeneous formation (cf. Table 1). Cases D-F are studied by the Monte Carlo method (200 realisations each). The realisations of case D are generated with an ordinary random number generator, whereas the realisations in cases E and F are generated with the turning bands method using an isotropic and exponential variogram model. For case D, $R_Y \approx \Delta x = \Delta y = 3$ m, and for cases E and F, $R_Y \approx 3\ \lambda_Y$.

	T_W (m²/s)	T_F (m²/s)	λ_Y (m)	R_Y (m)	$\langle T_m \rangle$ (m²/s)	$\langle r_{e,ave} \rangle$ (m)
B:	$\mathbf{10^{-7}}$	$\mathbf{10^{-7}}$	∞	∞	$\mathbf{8.58 \cdot 10^{-8}}$ (T_m)	**12.5** (r_e)
D:	10^{-7}	$\sim 10^{-7}$ (median)	-	3	$8.81 \cdot 10^{-8}$	11.5
E:	10^{-7}	$\sim 10^{-7}$ (median)	6	18	$8.15 \cdot 10^{-8}$	12.4
F:	10^{-7}	$\sim 10^{-7}$ (median)	12	36	$8.11 \cdot 10^{-8}$	12.9

Figure 21 yields that: (*i*) the variability of $r_{e,ave}$ is sensitive to the value of R_Y, whereas the variability of T_m is comparatively insensitive, and (*ii*) the distributions of $r_{e,ave}$ are fairly symmetric or slightly skewed to the right, whereas the distributions of T_m are all clearly skewed to the left. Figure 22 shows the three histograms of T_m in detail. The skewness suggests that the interpretation of T_m is sensitive to hydraulic resistances. In other words, radial flow to/from a point source is in some sense related to serial flow because T_m may

be a "low-valued" estimate of the spatially varying transmissivity conditions. (In serial flow the equivalent, or effective, transmissivity is equal to the harmonic mean.)

The histogram of $r_{e,std}$ in Figure 23 reveals that the envelope of the radius of influence for case E ($R_Y \approx 18$ m) is irregular with an ensemble mean value of $\langle r_{e,std} \rangle = 3.40$ m. (For a homogeneous formation $r_{e,std} = 0$ m.) The scatter diagram in Figure 23 reveals that the expected value and the variance of the irregularity increases with increasing value of $r_{e,ave}$. The scatter diagrams in Figure 24 show the irregularity of the envelope in terms of $r_{e,max}$ and $r_{e,min}$ for cases D-F in Tables 2 and 3. The scatter diagrams show that the expected value to the ratio $r_{e,max}/r_{e,min}$ is approximately greater than or equal to 2 regardless of the statistical structure imposed. It is only for small values of r_e that $r_{e,max} \approx r_{e,min}$.

Figure 25 shows two plots of $r_{e,ave}$ versus T_m for three different values of T_W. The two plots refer to cases G-I in Table 2. The regression line (solid) in the lower plot in Figure 25 yields that the coefficient of determination is 92% using an exponential regression model with $r_e \propto (T_m)^{0.31}$. The two pairs of dashed lines show the 95% confidence intervals for the fitted model and new observations, respectively. The good fit is an important result considering our previous discussion about the possibility for a $r_e \propto \sqrt[3]{T}$ relationship based on the linear relationship between $log_{10}(T)$ and $log_{10}(S)$ assumed in Figure 14. Firstly, it verifies the capability of the numerical model for dealing with high transmissivity contrasts. Secondly, it implies that simple analytical formulae derived for homogeneous media are of interest for heterogeneous media as well, e.g.., the regression line compares well with equation (9). By way of conclusion, the mean hydraulic behaviour of the heterogeneous formations dealt with in this study is unchanged and it resembles the hydraulic behaviour of the corresponding homogeneous case. It must not be forgotten that the results derived here apply to a multinormal distribution for $ln(T)$. The assumption of a multinormal distribution can be investigated by calculating the indicator variograms for different transmissivity thresholds (cf. Winberg, 1989). However, we argue that it is important to first verify that the double-packer tests as such are correctly interpreted.

The most important implication of the Monte Carlo results is that the support scale of double-packer tests in a heterogeneous medium is demonstrated to be a random variable, which is affected by both the hydraulic and statistical characteristics of the heterogeneous medium. This conclusion is in clear contradiction to what is tacitly assumed in present applications of the stochastic continuum analogue to flow in fractured hard rocks (see, e.g., Neuman, 1988; Winberg *et al.*, 1990). If the results derived in this study are general, the traditional methods for scaling-up, assuming a constant scale of support and a multinormal distribution for $ln(T)$, may lead to an underestimation of the persistence and connectivity of transmissive zones.

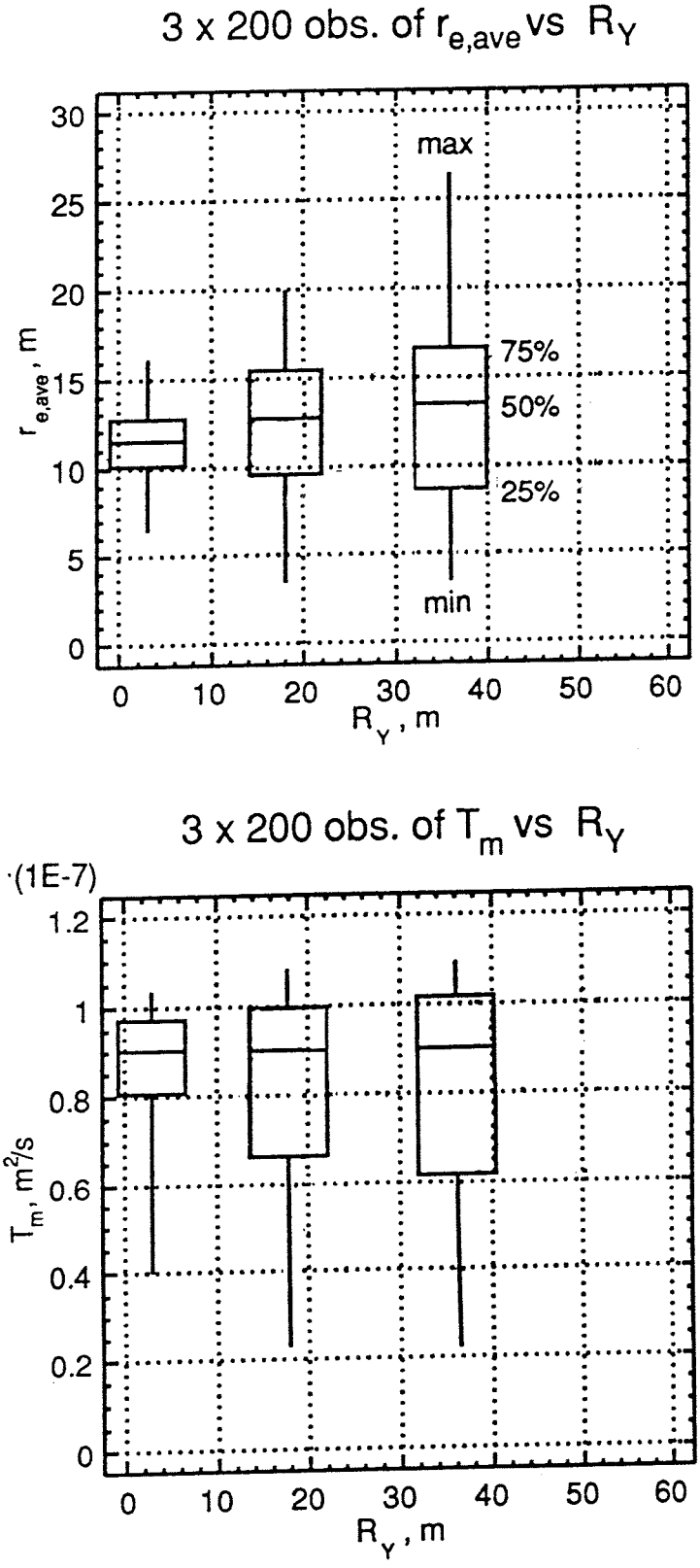

Fig. 21 Box plots of $r_{e,ave}$ vs. R_Y and T_m vs. R_Y for cases D-F ($R_Y \approx 3$ m, 18 m, and 36 m), see Table 3.

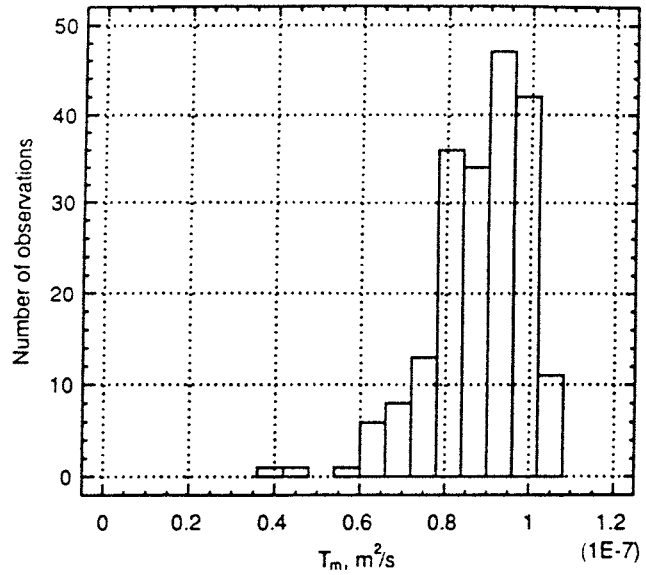

Case D:

$R_Y = 3$ m

$T_W = 10^{-7}$ m²/s

$\langle T_F \rangle = 10^{-7}$ m²/s
(ensemble median)

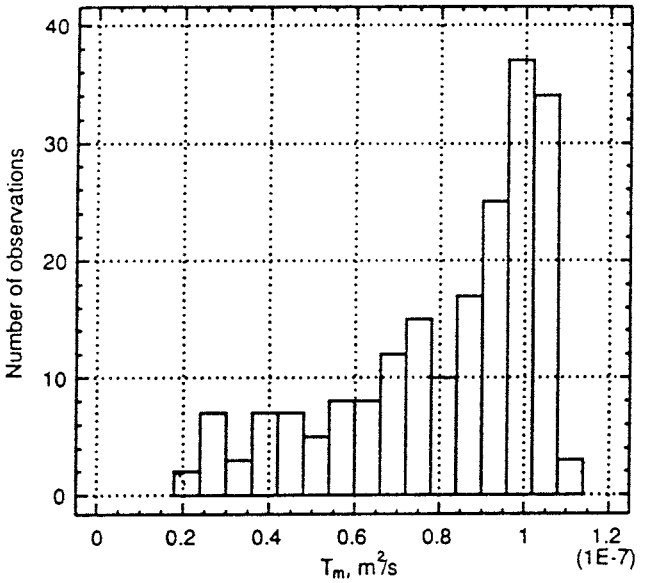

Case E:

$R_Y = 18$ m

$T_W = 10^{-7}$ m²/s

$\langle T_F \rangle = 10^{-7}$ m²/s
(ensemble median)

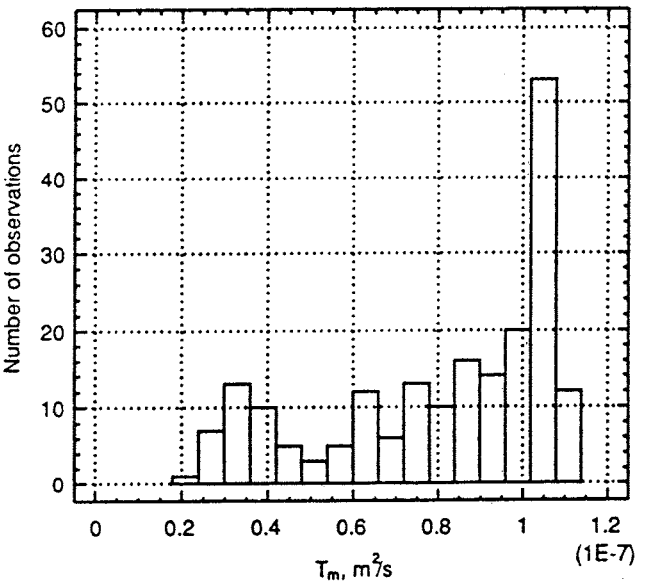

Case F:

$R_Y = 36$ m

$T_W = 10^{-7}$ m²/s

$\langle T_F \rangle = 10^{-7}$ m²/s
(ensemble median)

Fig. 22 Histograms of T_m for cases D-F ($R_Y \approx 3$ m, 18 m, and 36 m), see Table 3.

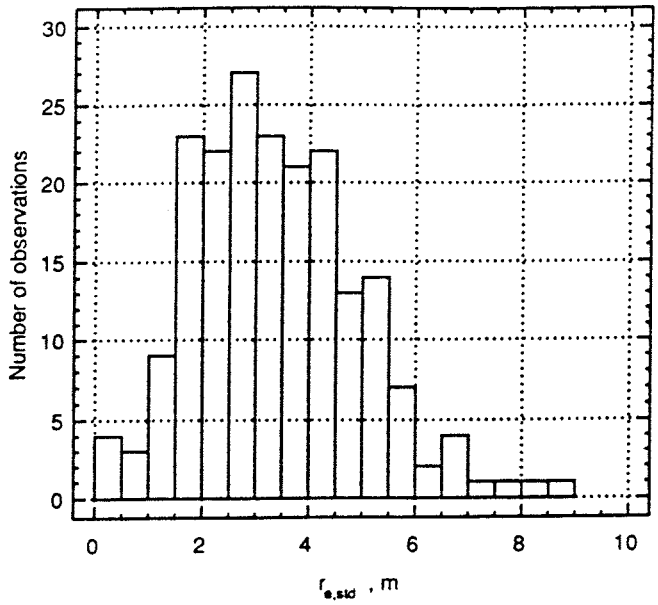

Case E:

$R_Y = 18$ m

$T_W = 10^{-7}$ m^2/s

$\langle T_F \rangle = 10^{-7}$ m^2/s
(ensemble median)

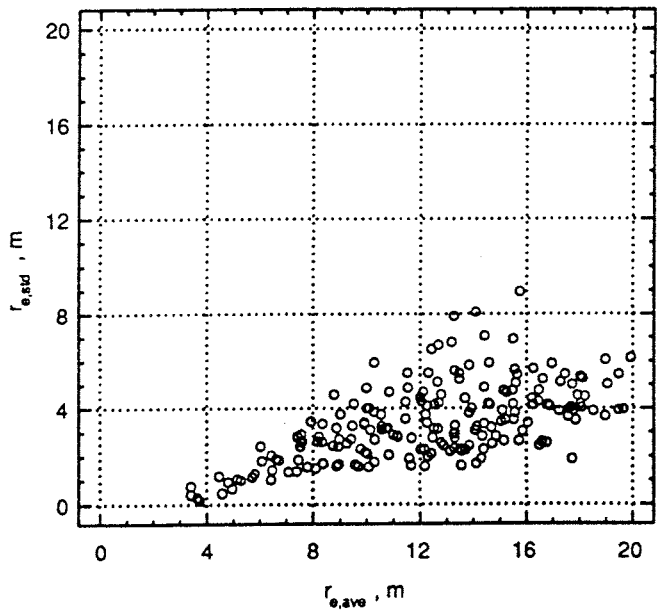

Fig. 23 Histogram of $r_{e,std}$ (top) and scatter diagram of $r_{e,std}$ vs. $r_{e,ave}$ (bottom) for case E ($R_Y \approx 18$ m), see Table 3.

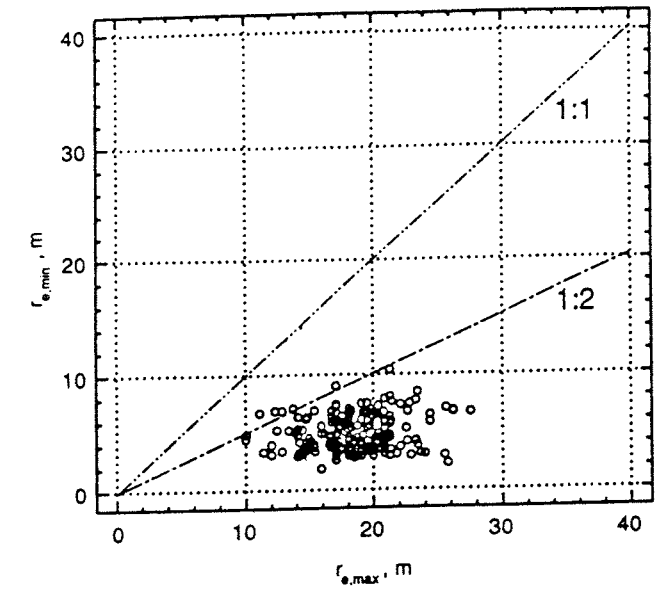

Case D:

R_Y = 3 m

$T_W = 10^{-7}$ m^2/s

$\langle T_F \rangle = 10^{-7}$ m^2/s
(ensemble median)

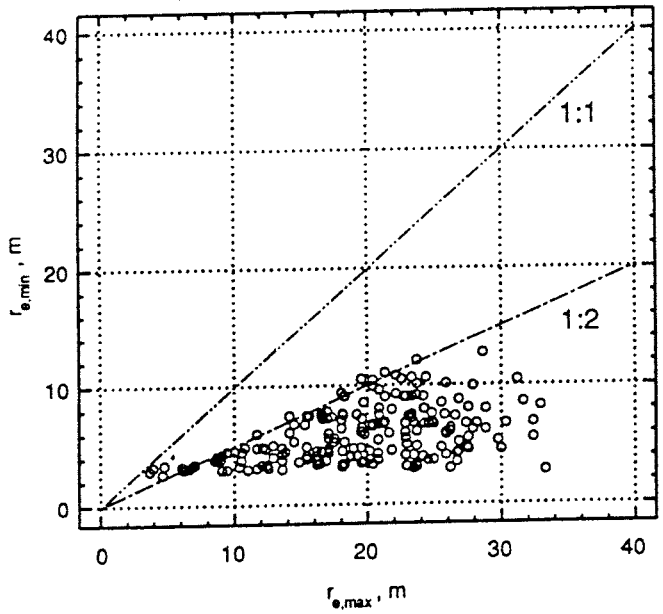

Case E:

R_Y = 18 m

$T_W = 10^{-7}$ m^2/s

$\langle T_F \rangle = 10^{-7}$ m^2/s
(ensemble median)

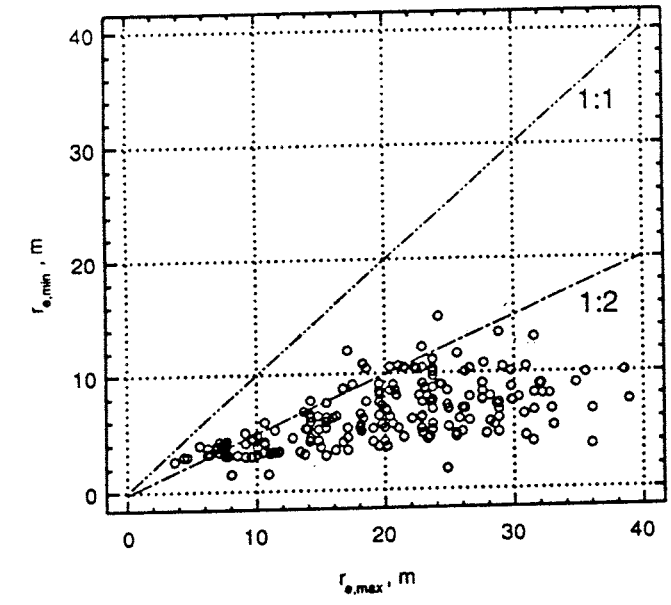

Case F:

R_Y = 36 m

$T_W = 10^{-7}$ m^2/s

$\langle T_F \rangle = 10^{-7}$ m^2/s
(ensemble median)

Fig. 24 Scatter plots of $r_{e,min}$ vs. $r_{e,max}$ for cases D-F ($R_Y \approx$ 3 m, 18 m, and 36 m), see Table 3

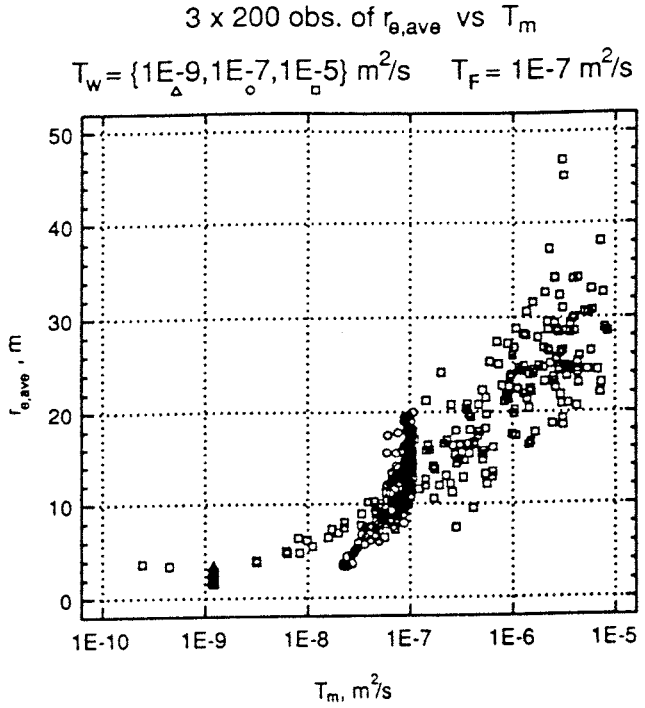

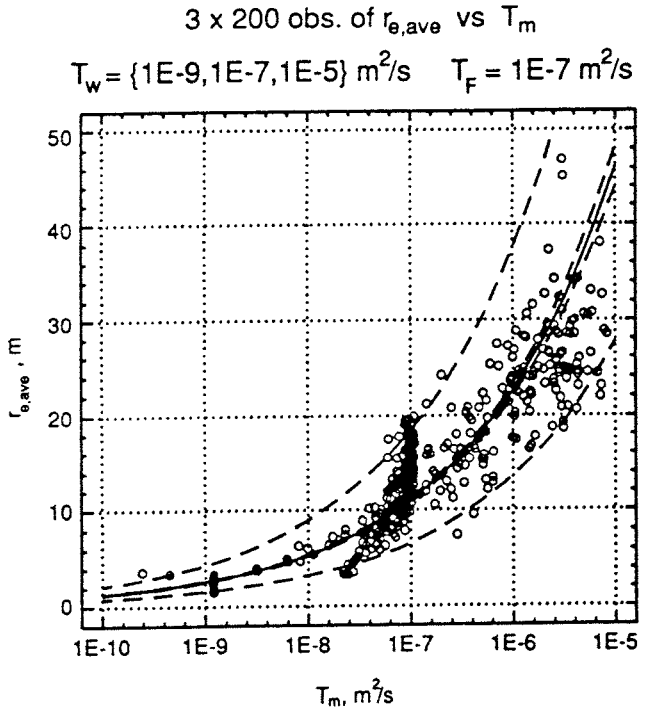

Fig. 25 Scatter plot of $r_{e,ave}$ vs. T_m (top) and regression of $r_{e,ave}$ on T_m (bottom). Both plots refer to cases G-I ($R_Y \approx 18$ m; $T_W = 10^{-9}$, 10^{-7}, and 10^{-5} m^2/s), see Table 2. In the upper plot, cases G-I are showed separately. In the lower plot, cases G-I are treated as one set of data. The innermost pair of dashed lines shows the 95% confidence interval for the fitted model (solid line). The outermost pair of dashed lines shows the 95% confidence interval for new observations.

Chapter 7

Conclusions

A two-dimensional numerical flow model is used to investigate the transmissivity and the radius of influence of single-hole double-packer tests in highly heterogeneous porous media. The spatial variability of $ln(T)$ is assumed to be multinormal on a 3 m scale. The experimental set-up used corresponds to a 15 minutes long constant-head injection test in a slim core borehole, which is a common single-hole test procedure within the Swedish nuclear waste repository programme in fractured hard rocks. The conclusions drawn can be summarised as follows:

(*a*) a positive borehole skin has severe effects on the transmissivity value interpreted as well as the corresponding radius of influence
(*b*) the transmissivity value interpreted is a complex average of the heterogeneity
(c) the corresponding radius of influence is irregular and of random nature
(*d*) the a priori assumption of an essentially radial flow regime, as implied by the traditional interpretation formulae used, e.g., Moye (1967), Cooper and Jacob (1946) and Jacob and Lohman (1952), is questioned
(*e*) the mean values of the transmissivity and the radius of influence of a double-packer test in a heterogeneous medium equal the transmissivity and the radius of influence of a similar test in a comparative homogeneous medium

Beginning with the interpretation of transmissivity, we conclude that the hydraulic conditions close to the borehole are extremely important considering the short test period used (15 minutes). For a transmissivity value of 10^{-9} m^2/s (or less) in the immediate vicinity of the borehole ($\leq$1.5 m), it is impossible to tell whether the surrounding formation is homogeneous or heterogeneous. Thus, if the flow capacity close to the borehole is altered by features that cause a positive skin such as clogging drilling debris, subsequent discrete fracture network transmissivity calibrations as well as porous media transmissivity interpretations, geostatistical analyses and conditional simulations will be distorted. Conversely, if the flow capacity is altered by features that cause a negative skin such as hydraulic fracturing, the aforementioned methods of analysis will reflect some kind of average of nearby and distant hydraulic conditions. In other words, the scale of support is varying.

The sensitivity of transmissivity interpretations to hydraulically resistive regions demonstrated in this study suggests that flow to/from a point source in a two-dimensional heterogeneous domain in some sense is related to serial flow. If this observation is correct it implies that the transmissivity value interpreted in conjunction with a single-hole double-packer test may be "low-valued" estimate of the spatially varying transmissivity conditions of the surrounding formation (cf. harmonic mean in serial flow). The implications of this conclusion are debatable from a safety assessment point of view, because the transmissivity value interpreted may not be a conservative estimate of the transmissivity for a non-radial flow regime.

The fact that the lateral support scale of field measurements is not a constant but a random variable is clearly demonstrated in this study by means of the Monte Carlo method. The results show that the radius of influence is affected by both the hydraulic and statistical characteristics of the heterogeneous medium. This conclusion is in clear contradiction to what is tacitly assumed in present applications of stochastic continuum concepts for flow and mass transport in porous media as well as in fractured hard rocks. If the results derived in this study are general, the traditional methods used for scaling-up, assuming a constant lateral scale of support and a multinormal distribution, may lead to an underestimation of the persistence and connectivity of transmissive zones. This might perhaps be of limited importance in conventional porous media applications of moderate heterogeneity, but not for assessing the post-closure radiological safety of a deep repository for high-level nuclear waste in highly heterogeneous media such as fractured hard rocks.

The two methods used in this study for interpreting constant-head injection tests, namely Moye's formula for steady-state analyses and Jacob-Lohman's formula for transient analyses, should compare fairly well only for a truly radial flow regime to/from a borehole without skin effects in a perfectly homogeneous formation (see, e.g., Black and Barker, 1987). This result is also reproduced in the present study using the numerical flow model. However, steady-state and transient interpretations of real tests differ in what seems to be a random fashion. For the particular borehole discussed in this study, namely KAS03 at the Äspö Hard Rock Laboratory in Sweden, the maximum difference is about one order of magnitude. The numerical simulations undertaken in this study show that varying skin effects alone cannot explain the random differences observed. Therefore, we conclude that the a priori assumption of an essentially radial flow regime, as implied by the interpretation formulae used, must be put in question.

This conclusion is supported by the results of, for example, Braester and Thunvik (1982, 1984), Barker (1988), and Geier and Doe (1992). Braester and Thunvik (1982, 1984) concluded that for short test section lengths, the flow regime around a borehole in a porous medium deviates from being radial to become somewhat more spherical. Transient

interpretation methods such as Jacob-Lohman's or Cooper-Jacob's formulae assume a perfectly radial flow regime, whereas Moye's formula is more adaptive to a radial-spherical flow regime. Thus, for non-radial flow regimes, results computed with Moye's and Jacob-Lohman's (or Cooper-Jacob's) formulae do not necessarily compare. Geier and Doe (1992) compared interpretations made with Moye's formula with interpretations made with the fractional dimension theory (Barker, 1988) for a number of double-packer test data from the Finnsjön study area in Sweden. They concluded that the two methods compare well in many cases but that significant deviations can occur in situations where the flow dimension is close to unity, e.g., a situation where an impervious rock mass is intersected by a single channel of high transmissivity.

An important result of the Monte Carlo simulations is that the mean values of the transmissivity and the radius of influence of double-packer tests in a heterogeneous medium equals the transmissivity and the radius of influence of a similar test in a comparative homogeneous medium. This result suggests that analytical formulae derived for homogeneous media are of interest. The difference between purely random and correlated fields shows up in terms of larger variances for the correlated fields. It is important to keep in mind that these observations are made for a multinormal type of heterogeneity.

Chapter 8

Discussion

Many geostatistical concepts used for generating random fields as input to numerical flow models origin from techniques developed for mineral exploration. In mining geostatistics, basic statistical prerequisites such as independent observations and a constant scale of support are fulfilled in the analyses of cores. However, in applications that use data of a varying lateral support, which is the general case in hydrogeological problems that use hydraulic data from boreholes, the adaptation of the traditional geostatistical methods is not evident. Nevertheless, this is exactly what is tacitly assumed in many applications of the stochastic continuum analogue to flow in fractured hard rocks (see, e.g., Neuman, 1988; Gustafson *et al.*, 1989; Winberg *et al.*, 1990; Svensson, 1991; Norman, 1992). In the work of Norman (1992) an approach to deal with packer-test data on multiple scales is suggested and applied to field data from fractured hard rocks. However, the approach suggested does not take a varying lateral support into account. Follin (1992) showed that statistical regularisation of hydraulic properties in highly heterogeneous porous media is a delicate matter because the relation to the original problem is easily lost.

With reference to the results of the present study concerning the varying lateral scale of support, i.e., radius of influence, we disagree with the traditional treatment for generating a heterogeneous hydraulic conductivity field on a large scale. The technique used for generating a heterogeneous hydraulic conductivity field on a large scale is debatable. It is based on the tacit assumption that the heterogeneity observed on a small scale, as determined by fixed-interval transmissivity measurements in single-hole core boreholes, is of constant lateral support. Furthermore, it is assumed that the transmissivities can be transformed to hydraulic conductivities and correctly regularised to a simple log-normal frequency distribution with a support scale that fits a given numerical discretisation. Using the results obtained in this study means that statistical regularisation should be avoided, i.e., the heterogeneous observed on a small scale should be generated "as is". Concerning the resulting computational constraints, we suggest that the coarser numerical discretisation should be governed by hydraulic principles rather than, as now, by statistical assumptions and traditional numerical modelling techniques. We argue that groundwater flow and advective mass transport from a repository located in a comparatively impervious

rock mass to a major fracture zone is governed by the most transmissive structures on that scale. Thus, the most transmissive structures should not be smeared out but treated as a second-order system of "fracture zones". (The second-order system is random, whereas the first-order system is deterministic and defined by the conceptual geological model.) The heterogeneous flow domain should be discretised numerically in a manner that maintains the persistence and connectivity of the second-order zones, whereas the intervening resistive regions are lumped into more or less impervious blocks. Because the configuration of the second-order system is random, the Monte Carlo method must be used to evaluate the effect of the corresponding uncertainty. Moreover, as the configuration of the heterogeneity varies between the realisations, the numerical discretisation will need to be specified afresh.

There are two main problem with the approach suggested. The first problem is to develop a technique that takes a varying lateral support scale into account while generating the random field. A tentative approach is to develop a hybrid of the sequential indicator simulation algorithm (Gómez-Hernández and Srivastava, 1990). One of the many attractive features of this algorithm is that different correlation lengths can be used simultaneously. Concerning the problem of numerical discretisation, Follin (1992) presented a numerical technique that automatically discretises a highly heterogeneous porous medium in two- or three dimensions according to a prescribed cutoff conductivity value. For a highly heterogeneous porous medium in two-dimensions, such as the one studied in this study, Follin (1992) concluded that the main flow and transport properties are preserved despite a frequency distribution cutoff of 25%. Further, the critical cutoff value for the a two-dimensional flow problem was found to be about 38%, which compares well with the critical probability for the two-dimensional site percolation problem on a square lattice, which is estimated to 38.2% (see, e.g., Piggott and Elsworth, 1992). For the three-dimensional site percolation problem on a cube lattice the critical probability is estimated to 71.8% (see, e.g., Piggott and Elsworth, 1992).

Nomenclature

A	= Area	[L^2]
b	= Thickness	[L]
C	= Covariance model of Y	[$ln^2(L^2T^{-1})$]
$[C]$	= Capacitance matrix	
$\{F\}$	= Specified flow matrix	
g	= Acceleration due to gravity	[LT^{-2}]
H	= Excess injection hydraulic head	[L]
h	= Hydraulic head	[L]
h	= Magnitude of a two-point Cartesian separation vector	[L]
$\{h\}$	= Hydraulic head matrix	
K	= Hydraulic conductivity	[LT^{-1}]
$[K]$	= Conductance matrix	
$\widetilde{k}$	= Permeability tensor	[L^2]
L	= Length of test section	[L]
p_w	= Water pressure	[$ML^{-1}T^{-2}$]
Q	= Volumetric flow rate	[L^3T^{-1}]
q	= Specific discharge	[LT^{-1}]
R_Y	= Correlation range of Y	[L]
r	= Radius	[L]
r_e	= Radius of influence	[L]
$r_{e,ave}$	= Mean value of the radius of influence	[L]
$r_{e,std}$	= Standard deviation value of the radius of influence	[L]
$r_{e,max}$	= Maximum value of the radius of influence	[L]
$r_{e,min}$	= Minimum value of the radius of influence	[L]
r_w	= Borehole radius	[L]
r_ξ	= Skin zone radius	[L]
S	= Storativity	[-]
S_s	= Specific storage	[L^{-1}]
S_{ref}	= Storativity of reference case	[L^{-1}]
T	= Transmissivity	[L^2T^{-1}]
T_F	= Median transmissivity of a heterogeneous medium	[L^2T^{-1}]
T_G	= Median transmissivity of $exp(Y)$	[L^2T^{-1}]
T_c	= Cooper-Jacob's transmissivity	[L^2T^{-1}]

T_j	= Jacob-Lohman's transmissivity	[L^2T^{-1}]
T_m	= Moye's transmissivity	[L^2T^{-1}]
T_{ref}	= Transmissivity of reference case	[L^2T^{-1}]
T_W	= Borehole block transmissivity	[L^2T^{-1}]
T_Z	= Fracture zone transmissivity	[L^2T^{-1}]
T_ξ	= Skin zone transmissivity	[L^2T^{-1}]
t	= Time	[T]
t_D	= Dimensionless time	[-]
x	= Cartesian coordinate	[L]
y	= Cartesian coordinate	[L]
Y	= $ln(T)$	[$ln(L^2T^{-1})$]
z	= Cartesian coordinate	[L]
$\hat{z}$	= Unit vector in the z direction	[L]
ϕ	= Effective porosity of porous medium	[-]
λ_Y	= Parameter for an exponential covariance model of Y	[L]
μ_w	= Dynamic viscosity of water	[$ML^{-1}T^{-1}$]
ρ_w	= Water density	[ML^{-3}]
σ_Y	= Standard deviation of Y	[$ln(L^2T^{-1})$]
ξ	= Borehole skin	[-]
∇	= Gradient operator	
∂	= Partial derivative operator	
$\langle\ \rangle$	= Expectation operator	

References

Almén, K. E., J. E. Andersson, L. Carlsson, K. Hansson, and N. Å. Larsson (1986) Hydraulic testing in crystalline rock: A comparative study of single hole test methods, *SKB Technical Report TR 86-27*, Stockholm.

Andersson, J. E., L. Ekman and A. Winberg (1988) Detailed hydraulic characterization of a fracture zone in the Brändan area, Finnsjön, Sweden, *4th Can./Am. Conf. on Hydrogeology: Fluid Flow, Heat Transfer and Mass Transport in Fractured Rocks*, Banff, Alta., 21-24 June, Alberta Research Council and the Association of Groundwater Scientists and Engineers (Div. NWWA), Alberta.

Ball, J. K., J. H. Black, M. Brightman and T. W. Doe Large scale cross hole testing, *OECD/NEA Internal Report of the Stripa Project TR 91-17*, SKB, Stockholm.

Barenblatt, G. E., I. P. Zheltov and I. N. Kochina (1960) Basic concepts in the theory of seepage of homogeneous liquids in fissured rocks, *J. Appl. Math. Mech.*, 24(5), 1286-1303. (English translation.)

Barker, J. A. (1988) A generalized radial flow model for hydraulic tests in fractured rock, *Water Resour. Res.*, 24(10), 1796-1804.

Bear, J. (1972) *Dynamics of Fluids in Porous Media*, American Elsevier, New York.

Black, J. H. and J. A. Barker (1987) Design of Single-Borehole Hydraulic Test Programme Allowing for Interpretation-Based Errors, *Nagra Technical Report 87-03*, Baden.

Braester, C. and R. Thunvik (1982) Numerical simulation of double-packer tests. Calculation of rock permeability, *SKB Technical Report TR 82-06*, Stockholm.

Braester, C. and R.Thunvik (1984) Determination of formation permeability by double-packer tests, *J. of Hydrology*, 72, 375-389.

Cacas, M.C., E. Ledoux, G. de Marsily, B. Tillie, A. Barbreau, E. Durand, B. Fuega and P. Peaudecerf (1990a) Modelling fracture flow with a stochastic discrete fracture model: Calibration and validation, 1. The flow model, *Water Resour. Res.*, 26(3), 479-489.

Cacas, M.C., E. Ledoux, G. de Marsily, A. Barbreau, P. Camels, B. Gaillard and R. Margitta (1990b) Modelling fracture flow with a stochastic discrete fracture model: Calibration and validation, 2. The transport model, *Water Resour. Res.*, 26(3), 491-500.

Carlsson, A. and T. Olsson (1981) Hydraulic properties of a fractured granitic rock mass at Forsmark, Sweden, *Swedish Geological Survey, Series C783*, Uppsala.

Carlsson, L., B.Gentzschein, G. Gidlund, K. Hansson, T. Svenson and U. Thoregren (1980) Kompletterande permeabilitetsmätningar i finnsjöområdet, *SKB Technical Report TR 80-10*, Stockholm. (In Swedish.)

Cooper, H. H. Jr. and C. E. Jacob (1946) A generalized graphical method for evaluating formation constants and summarizing well field history, *Trans. Am. Geophys. Un.*, 27, 526-534.

Cvetkovic, V. and C. S. Kung (1989) Variogram analysis of single-hole packer test data from the Finnsjön site, *SKB Arbetsrapport AR 89-17*, Stockholm.

Dagan, G. (1978) A note on packer, slug, and recovery tests in unconfined aquifers, *Water Resour. Res.*, 14(5), 929-934.

Dagan, G. (1982) Stochastic modeling of groundwater flow by unconditional and conditional probabilities, 1. Conditional simulation and the direct problem, *Water Resour. Res.*, 18(4), 813-833.

Delhomme, J. P. (1979) Spatial variability and uncertainty in groundwater flow parameters: A geostatistical approach, *Water Resour. Res.*, 15(2), 269-280.

Dershowitz, W. S. (1985) Rock joint systems, PhD thesis, Massachusetts Institute of Technology, Cambridge.

Doe, T. W. and J. E. Geier (1990) Interpretation of fracture system geometry using well test data, *OECD/NEA Internal Report of the Stripa Project TR 91-03*, SKB, Stockholm.

Doe, T. W. and J.S. Remer (1981) Analysis of constant-pressure well tests in nonporous fractured rock, *Proc. of the Third Invitational Well-Testing Symposium - Well Testing in Low-Permeability Environments*, (March-26-28, 1980), University of California, Lawrence Berkeley, Laboratory, Berkeley.

Duguid, J. O. and P. C. Y. Lee (1977) Flow in fractured porous media, *Water Resour. Res.*, 13(3), 558-566.

Duff, I. S. (1981) MA32 - A package for solving sparse unsymmetric systems using the fronal method, *UKAEA Report AERE - R10079*, Oxfordshire.

Dverstorp, B. (1991) Analyzing flow and transport in fractured rock using the discrete fracture network concept, PhD thesis, Royal Institute of Technology, *TRITA-VBI-151*, Stockholm.

Earlougher, R. C., Jr. (1977) *Advances in Well Test Analysis*, SPE AIME, Dallas.

Follin, S. (1992) Numerical calculations on heterogeneity of groundwater flow, PhD thesis, *SKB Technical Report TR 92-14*, Stockholm.

Freeze, R. A. (1975) A stochastic-conceptual analysis of one-dimensional ground water flow in nonuniform homogeneous media, *Water Resour. Res*, 11(5), 725-741.

Freeze, R. A., J. Massman, L. Smith, T. Sperling and B. James (1990) Hydrogeological decision analysis: 1. A framework, *Ground Water*, 28 (5), 738-766.

Geier, J. E. and C. L. Axelsson (1991) Discrete fracture modelling of the Finnsjön rock mass, Phase 1: Feasibility study, *SKB Technical Report TR 91-13*, Stockholm.

Geier, J. E., C. L. Axelsson, L. Hässler and A. Benabderrahmane (1992) Discrete fracture modelling of the Finnsjön rock mass, Phase 2, *SKB Technical Report TR 92-07*, Stockholm.

Geier, J. E. and T. W. Doe (1992).Discrete fracture modelling of the Finnsjön rock mass - Supplementary interpretations of actual and simulated well test data, *SKB Arbetsrapport AR 92-45*, Stockholm.

Gómez-Hernández, J. J. and R. M. Srivastava, ISIM3D: An ANSI-C three-dimensional multiple indicator conditional simulation program, *Computer and Geosciences*, 16(4), 395-440, 1990.

Gustafson, G., R. Stanfors and P. Wikberg (1989) Swedish Hard Rock Laboratory Evaluation of 1988 year preinvestigations and description of the target area of Äspö, *SKB Technical Report TR 89-16*, Stockholm.

Holmes, D. C. (1989) Site characterization and validation - Single borehole hydraulic testing, Stage 1, *OECD/NEA Internal Report of the Stripa Project TR 89-04*, SKB,Stockholm.

Hvorslev, M. J. (1951) Time lag and soil permeability in groundwater observations, *U.S. Army Corps Eng., Bull. 36*, Waterways Exp. Stn., Vicksburg, Miss.

Hubbert, M K. (1956) Darcy law and the field equations of flow of the underground fluids, *Trans. Am. Inst. Min. Metall. Pet. Eng.*, 207, 222-239.

Jacob, C. E. (1950) Flow of Groundwater, In: Rouse, H. (ed.) *Engineering Hydraulics*, Chap. 5, 321-386, Wiley, New York.

Jacob, C. E. and S. Lohman (1952) Nonsteady flow to a well of constant drawdown in an extensive aquifer, *Trans. Am. Geophys. Union*, 33(4), 559-569.

Liedholm, M. (1991a) Conceptual Modeling of Äspö Technical Notes 1-17, *SKB Progress Report 25-90-16a*, Stockholm.

Liedholm, M. (1991b) Conceptual Modeling of Äspö Technical Notes 18-32, *SKB Progress Report 25-90-16b*, Stockholm.

Long, J. C. S., J. S. Remer, C. R. Wilson and P. A. Witherspoon (1982) Porous media equivalents for networks of discontinuous fractures, *Water Resour. Res.*, 18(3), 645-658.

Mantoglou, A. and J. L. Wilson (1982) The turning bands method for simulation of random fields using line generation by a spectral method, *Water Resour. Res.*, 18(5), 1379-1394.

Marsily, G. de (1986) *Quantitative Hydrogeology*, Academic Press, Orlando.

Moye, D. G. (1967) Diamond drilling for foundation exploration, *Civ. Eng. Trans. 7th Inst. Eng. Australia*, 95-100.

Neuman, S.P. (1987) Stochastic continuum representation of fractured rock permeability as an alternative to the REV and fracture network concepts, In: Farmer, I. W. *et al.* (eds.) *Proc. 28th U.S. Symp. Rock Mech.*, 553-561, Balkema, Rotterdam.

Neuman, S.P. (1988) A proposed conceptual framework and methodology for investigatingflow and transport in Swedish crystalline rocks, *SKB Arbetsrapport AR 88-37*, Stockholm.

Nilsson, L. (1989) Hydraulic tests at Äspö and Laxemar - Evaluation, *SKB Progress Report 25-88-14*, Stockholm.

Nilsson, L. (1990) Hydraulic test at Äspö - KAS05-KAS08, HAS13-HAS17, *SKB Progress Report 25-89-20*, Stockholm.

Norman, S. (1992) Statistical inference and comparison of stochastic models for the hydraulic conductivity at the Finnsjön-site, *SKB Technical Report TR 92-08*, Stockholm.

Peck, N.J., S. Gorelick, G. de Marsily, S. Foster and V. Kovalevsky (1988) *Consequences of Spatial Variability in Aquifer Properties and Data Limitations for Groundwater Modelling Practice, 175*, IAH Press, Oxfordshire.

Piggott, A. R. and D. Elsworth (1992) Analytical models for flow through obstructed domains, *J. Geoph. Res.*, 97(B2), 2085-2093.

Robinson, P. C. (1984) Connectivity, flow and transport in network models of fractured media, PhD thesis, *Theor. Phys. Div. TP. 1072*, AERE Harwell, Oxfordshire.

Schrage, L. (1969) A more portable FORTRAN random number generator, *ACM Trans. on Mathematical Software*, 5(2), 132-138.

Stokes, J. (1980) On the description of the properties of fractured rock using the concept of a porous medium, *SKB Technical Report TR 80-05*, SKB, Stockholm.

Svensson, U. (1991) Groundwater flow at Äspö and changes due to the excavation of the laboratory, *SKB Progress Report 25-91-03*, Stockholm.

Tsang, Y. W. and C. F. Tsang (1989) Flow channeling in a single fracture as a two-dimensional strongly heterogeneous porous medium, *Water Resour. Res.*, 25(9), 1076-1080.

Thiem, G. (1906) *Hydrologische Methoden*, J. M. Gebhardt, Leibzig.

Warren, J.E. and P. J. Root (1963) The behaviour of naturally fractured reservoirs, *Soc. Pet. Eng. J.*, 1, 153-169.

Winberg, A. (1989) Project 90 - Analysis of spatial variability of hydraulic conductivity data in the SKB data base GEOTAB, *SKI Technical Report TR 89-12*, Stockholm.

Winberg, A., C. S. Kung, X. H. Wen and V. Cvetkovic (1990) SKB 91 Stochastic Continuum modelling of mass arrival at Finnsjön - Parametric and non-parametric approaches, *SKB Arbetsrapport AR 90-40*, Stockholm.

Winberg, A. (1991) Analysis of spatial correlation of hydraulic conductivity data from the Stripa mine, *OECD/NEA Internal Report of the Stripa Project TR 91-28*, SKB, Stockholm.

List of SKB reports

Annual Reports

1977-78
TR 121
KBS Technical Reports 1 – 120
Summaries
Stockholm, May 1979

1979
TR 79-28
The KBS Annual Report 1979
KBS Technical Reports 79-01 – 79-27
Summaries
Stockholm, March 1980

1980
TR 80-26
The KBS Annual Report 1980
KBS Technical Reports 80-01 – 80-25
Summaries
Stockholm, March 1981

1981
TR 81-17
The KBS Annual Report 1981
KBS Technical Reports 81-01 – 81-16
Summaries
Stockholm, April 1982

1982
TR 82-28
The KBS Annual Report 1982
KBS Technical Reports 82-01 – 82-27
Summaries
Stockholm, July 1983

1983
TR 83-77
The KBS Annual Report 1983
KBS Technical Reports 83-01 – 83-76
Summaries
Stockholm, June 1984

1984
TR 85-01
Annual Research and Development Report 1984
Including Summaries of Technical Reports Issued during 1984. (Technical Reports 84-01 – 84-19)
Stockholm, June 1985

1985
TR 85-20
Annual Research and Development Report 1985
Including Summaries of Technical Reports Issued during 1985. (Technical Reports 85-01 – 85-19)
Stockholm, May 1986

1986
TR 86-31
SKB Annual Report 1986
Including Summaries of Technical Reports Issued during 1986
Stockholm, May 1987

1987
TR 87-33
SKB Annual Report 1987
Including Summaries of Technical Reports Issued during 1987
Stockholm, May 1988

1988
TR 88-32
SKB Annual Report 1988
Including Summaries of Technical Reports Issued during 1988
Stockholm, May 1989

1989
TR 89-40
SKB Annual Report 1989
Including Summaries of Technical Reports Issued during 1989
Stockholm, May 1990

1990
TR 90-46
SKB Annual Report 1990
Including Summaries of Technical Reports Issued during 1990
Stockholm, May 1991

1991
TR 91-64
SKB Annual Report 1991
Including Summaries of Technical Reports Issued during 1991
Stockholm, April 1992

Technical Reports

List of SKB Technical Reports 1992

TR 92-01
GEOTAB. Overview
Ebbe Eriksson[1], Bertil Johansson[2], Margareta Gerlach[3], Stefan Magnusson[2], Ann-Chatrin Nilsson[4], Stefan Sehlstedt[3], Tomas Stark[1]
[1]SGAB, [2]ERGODATA AB, [3]MRM Konsult AB
[4]KTH
January 1992

TR 92-02
Sternö study site. Scope of activities and main results
Kaj Ahlbom[1], Jan-Erik Andersson[2], Rune Nordqvist[2], Christer Ljunggren[3], Sven Tirén[2], Clifford Voss[4]
[1]Conterra AB, [2]Geosigma AB, [3]Renco AB,
[4]U.S. Geological Survey
January 1992

TR 92-03
Numerical groundwater flow calculations at the Finnsjön study site – extended regional area
Björn Lindbom, Anders Boghammar
Kemakta Consultants Co, Stockholm
March 1992

TR 92-04
Low temperature creep of copper intended for nuclear waste containers
P J Henderson, J-O Österberg, B Ivarsson
Swedish Institute for Metals Research, Stockholm
March 1992

TR 92-05
Boyancy flow in fractured rock with a salt gradient in the groundwater – An inititial study
Johan Claesson
Department of Building Physics, Lund University, Sweden
February 1992

TR 92-06
Characterization of nearfield rock – A basis for comparison of repository concepts
Roland Pusch, Harald Hökmark
Clay Technology AB and Lund University of Technology
December 1991

TR 92-07
Discrete fracture modelling of the Finnsjön rock mass: Phase 2
J E Geier, C-L Axelsson, L Hässler,
A Benabderrahmane
Golden Geosystem AB, Uppsala, Sweden
April 1992

TR 92-08
Statistical inference and comparison of stochastic models for the hydraulic conductivity at the Finnsjön site
Sven Norman
Starprog AB
April 1992

TR 92-09
Description of the transport mechanisms and pathways in the far field of a KBS-3 type repository
Mark Elert[1], Ivars Neretnieks[2], Nils Kjellbert[3], Anders Ström[3]
[1]Kemakta Konsult AB
[2]Royal Institute of Technology
[3]Swedish Nuclear Fuel and Waste Management Co
April 1992

TR 92-10
Description of groundwater chemical data in the SKB database GEOTAB prior to 1990
Sif Laurent[1], Stefan Magnusson[2], Ann-Chatrin Nilsson[3]
[1]IVL, Stockholm
[2]Ergodata AB, Göteborg
[3]Dept. of Inorg. Chemistry, KTH, Stockholm
April 1992

TR 92-11
Numerical groundwter flow calculations at the Finnsjön study site – the influence of the regional gradient
Björn Lindbom, Anders Boghammar
Kemakta Consultants Co., Stockholm, Sweden
April 1992

TR 92-12
HYDRASTAR – a code for stochastic simulation of groundwater flow
Sven Norman
Abraxas Konsult
May 1992

TR 92-13
Radionuclide solubilities to be used in SKB 91
Jordi Bruno[1], Patrik Sellin[2]
[1]MBT, Barcelona Spain
[2]SKB, Stockholm, Sweden
June 1992

TR 92-14
Numerical calculations on heterogeneity of groundwater flow
Sven Follin
Department of Land and Water Resources, Royal Institute of Technology
June 1992

TR 92-15
Kamlunge study site.
Scope of activities and main results
Kaj Ahlbom[1], Jan-Erik Andersson[2],
Peter Andersson[2], Thomas Ittner[2],
Christer Ljunggren[3], Sven Tirén[2]
[1]Conterra AB
[2]Geosigma AB
[3]Renco AB
May 1992

TR 92-16
Equipment for deployment of canisters with spent nuclear fuel and bentonite buffer in horisontal holes
Vesa Henttonen, Miko Suikki
JP-Engineering Oy, Raisio, Finland
June 1992

TR 92-17
The implication of fractal dimension in hydrogeology and rock mechanics
Version 1.1
W Dershowitz[1], K Redus[1], P Wallmann[1],
P LaPointe[1], C-L Axelsson[2]
[1]Golder Associates Inc., Seattle, Washington, USA
[2]Golder Associates Geosystem AB, Uppsala, Sweden
February 1992

TR 92-18
Stochastic continuum simulation of mass arrival using a synthetic data set.
The effect of hard and soft conditioning
Kung Chen Shan[1], Wen Xian Huan[1], Vladimir Cvetkovic[1], Anders Winberg[2]
[1] Royal Institute of Technology, Stockholm
[2] Conterra AB, Gothenburg
June 1992

TR 92-19
Partitioning and transmutation.
A review of the current state of the art
Mats Skålberg, Jan-Olov Liljenzin
Department of Nuclear Chemistry,
Chalmers University of Technology
October 1992

TR 92-20
SKB 91
Final disposal of spent nuclear fuel.
Importance of the bedrock for safety
SKB
May 1992

TR 92-21
The Protogine Zone.
Geology and mobility during the last 1.5 Ga
Per-Gunnar Andréasson, Agnes Rodhe
September 1992

TR 92-22
Klipperås study site.
Scope of activities and main results
Kaj Ahlbom[1], Jan-Erik Andersson[2],
Peter Andersson[2], Tomas Ittner[2],
Christer Ljunggren[3], Sven Tirén[2]
[1]Conterra AB
[2]Geosigma AB
[3]Renco AB
September 1992

TR 92-23
Bedrock stability in Southeastern Sweden. Evidence from fracturing in the Ordovician limestones of Northern Öland
Alan Geoffrey Milnes[1], David G Gee[2]
[1]Geological and Environmental Assessments (GEA), Zürich, Switzerland
[2]Geologiska Institutionen, Lund, Sweden
September 1992

TR 92-24
Plan 92
Costs for management of the radioactive waste from nuclear power production
Swedish Nuclear Fuel and Waste Management Co
June 1992

TR 92-25
Gabbro as a host rock for a nuclear waste repository
Kaj Ahlbom[1], Bengt Leijon[1], Magnus Liedholm[2],
John Smellie[1]
[1]Conterra AB
[2]VBB VIAK
September 1992

TR 92-26
Copper canisters for nuclear high level waste disposal. Corrosion aspects
Lars Werme, Patrik Sellin, Nils Kjellbert
Swedish Nuclear Fuel and Waste Management Co, Stockholm, Sweden
October 1992

TR 92-27

Thermo-mechanical FE-analysis of butt-welding of a Cu-Fe canister for spent nuclear fuel

B L Josefson[1], L Karlsson[2], L-E Lindgren[2], M Jonsson[2]
[1]Chalmers University of Technology, Göteborg, Sweden
[2]Division of Computer Aided Design, Luleå University of Technology, Luleå, Sweden
October 1992

TR 92-28

A rock mechanics study of Fracture Zone 2 at the Finnsjön site

Bengt Leijon[1], Christer Ljunggren[2]
[1]Conterra AB
[2]Renco AB
January 1992

TR 92-29

Release calculations in a repository of the very long tunnel type

L Romero, L Moreno, I Neretnieks
Department of Chemical Engineering,
Royal Institute of Technology, Stockholm, Sweden
November 1992

TR 92-30

Interaction between rock, bentonite buffer and canister. FEM calculations of some mechanical effects on the canister in different disposal concepts

Lennart Börgesson
Clay Technology AB, Lund Sweden
July 1992

TR 92-31

The Äspö Hard Rock Laboratory: Final evaluation of the hydro-geochemical pre-investigations in relation to existing geologic and hydraulic conditions

John Smellie[1], Marcus Laaksoharju[2]
[1]Conterra AB, Uppsala, Sweden
[2]GeoPoint AB, Stockholm, Sweden
November 1992

TR 92-32

Äspö Hard Rock Laboratory: Evaluation of the combined longterm pumping and tracer test (LPT2) in borehole KAS06

Ingvar Rhén[1] (ed.), Urban Svensson[2] (ed.), Jan-Erik Andersson[3], Peter Andersson[3], Carl-Olof Eriksson[3], Erik Gustafsson[3], Thomas Ittner[3], Rune Nordqvist[3]
[1]VBB VIAK AB
[2]Computer-aided Fluid Engineering
[3]Geosigma AB
November 1992

TR 92-33

Finnsjö Study site. Scope of activities and main results

Kaj Ahlbom[1], Jan-Erik Andersson[2], Peter Andersson[2], Thomas Ittner[2], Christer Ljunggren[3], Sven Tirén[2]
[1]Conterra AB
[2]Geosigma AB
[3]Renco AB
December 1992

TR 92-34

Sensitivity study of rock mass response to glaciation at Finnsjön, Central Sweden

Jan Israelsson[1], Lars Rosengren[1], Ove Stephansson[2]
[1]Itasca Geomekanik AB, Falun, Sweden
[2]Royal Institute of Technology, Dept. of Engineering Geology, Stockholm, Sweden
November 1992

TR 92-35

Calibration and validation of a stochastic continuum model using the Finnsjön Dipole Tracer Test. A contribution to INTRAVAL Phase 2

Kung Chen Shan[1], Vladimir Cvetkovic[1], Anders Winberg[2]
[1]Royal Institute of Technology, Stockholm
[2]Conterra AB, Göteborg
December 1992